Title

Scientific Findings to Engineering Realities: Coordination across Collab teams and making the connection to FORGE

Authors
Kneafsey, Timothy
Neupane, Ghanashyam
Blankenship, Douglas
et al.

Publication Date
2021-11-09

Scientific Findings to Engineering Realities

Coordination across Collab teams and making the connection to FORGE

Tim Kneafsey, Ghanashyam Neupane, Doug Blankenship, Patrick Dobson, Mark White, Joe Morris, Pengcheng Fu, Tim Johnson, Martin Schoenball, Jonathan Ajo-Franklin, Jon Weers and EGS Collab Team*

* J. Ajo-Franklin, T. Baumgartner, K. Beckers, D. Blankenship, A. Bonneville, L. Boyd, S. Brown, J.A. Burghardt, C. Chai, A. Chakravarty, T. Chen, Y. Chen, B. Chi, K. Condon, P.J. Cook, D. Crandall, P.F. Dobson, T. Doe, C.A. Doughty, D. Elsworth, J. Feldman, Z. Feng, A. Foris, L.P. Frash, Z. Frone, P. Fu, K. Gao, A. Ghassemi, Y. Guglielmi, B. Haimson, A. Hawkins, J. Heise, Chet Hopp, M. Horn, R.N. Horne, J. Horner, M. Hu, H. Huang, L. Huang, K.J. Im, M. Ingraham, E. Jafarov, R.S. Jayne, T.C. Johnson, S.E. Johnson, B. Johnston, S. Karra, K. Kim, D.K. King, T. Kneafsey, H. Knox, J. Knox, D. Kumar, K. Kutun, M. Lee, D. Li, J. Li, K. Li, Z. Li, M. Maceira, P. Mackey, N. Makedonska, C.J. Marone, E. Mattson, M.W. McClure, J. McLennan, T. McLing, C. Medler, R.J. Mellors, E. Metcalfe, J. Miskimins, J. Moore, C.E. Morency, J.P. Morris, T. Myers, S. Nakagawa, G. Neupane, G. Newman, A. Nieto, T. Paronish, R. Pawar, P. Petrov, B. Pietzyk, R. Podgorney, Y. Polsky, J. Pope, S. Porse, J.C. Primo, C. Reimers, B.Q. Roberts, M. Robertson, V. Rodriguez-Tribaldos, W. Roggenthen, J. Rutqvist, D. Rynders, M. Schoenball, P. Schwering, V. Sesetty, C.S. Sherman, A. Singh, M.M. Smith, H. Sone, E.L. Sonnenthal, F.A. Soom, D.P. Sprinkle, S. Sprinkle, C.E. Strickland, J. Su, D. Templeton, J.N. Thomle, C. Ulrich, N. Uzunlar, A. Vachaparampil, C.A. Valladao, W. Vandermeer, G. Vandine, D. Vardiman, V.R. Vermeul, J.L. Wagoner, H.F. Wang, J. Weers, N. Welch, J. White, M.D. White, P. Winterfeld, T. Wood, S. Workman, H. Wu, Y.S. Wu, E.C. Yildirim, Y. Zhang, Y.Q. Zhang, Q. Zhou, M.D. Zoback

November 9, 2021

Table of Contents

Executive Summary

This document provides a distillation of learnings of the EGS Collab (Collab) project for several topics of interest requested by the Utah Frontier Observatory for Research in Geothermal Energy (FORGE) project. This document was written following the completion of Collab Experiment 1, but prior to beginning Collab Experiment 2. Recommendations offered herein are perspectives offered by Collab scientists in support of FORGE.

The United States has an enormous indigenous renewable energy potential from enhanced geothermal systems (EGS). To realize this potential, the US Department of Energy (DOE) Geothermal Technologies Office (GTO) has made significant investments into research to eliminate impediments to developing EGS. Two major current projects are Collab initiated in 2017, and the FORGE project initiated with a site selection process in 2015.

Collab is a collaborative multi-national-lab, university, and commercial entity research endeavor bringing together a team of skilled and experienced subsurface process modeling, monitoring, and experimentation researchers and engineers to focus on intermediate-scale EGS reservoir creation processes and related model validation in crystalline rock. Collab is utilizing readily accessible underground facilities to refine the understanding of rock mass response to stimulation using experiments on the order of 10 m scale under EGS-relevant stress conditions. Experimental results from Collab stimulation, flow, tracer, and thermal tests are being used to validate coupled thermal-hydrological-mechanical-chemical (THMC) modeling approaches applicable to EGS. Collab is also testing and improving conventional and novel field monitoring tools. The project focuses on understanding and predicting permeability enhancement and evolution in crystalline rock. This focused research includes creating sustained and distributed permeability for heat extraction by generating new fractures that complement existing natural fractures.

FORGE has the mission of establishing an EGS field test site that enables cutting-edge research and testing for EGS technology to identify a replicable, commercial pathway to EGS. The FORGE team is developing the EGS field test site near Milford, Utah. The two projects differ in some attributes, including spatial scale (Collab / FORGE - 10-m / reservoir), access to the rock (short boreholes and nearby instruments / deep wells and standard field geophysical equipment), environmental conditions (cool rock at reasonable stress / hot rock at reasonable stress), focus (direct investigation / development of a testbed and management of a research program), and project structure (integrated team / science and engineering framework supporting many individual research teams).

The specific topics of this report requested by FORGE are: 1) data processing, annotation, and integration; 2) processing seismic data, 3) connecting geophysics, fractures, and flow systems, and 4) challenges of modeling fractured flow systems. Each of these topics is briefly discussed in this executive summary and covered in substantially greater detail in the main document. Numerous conference and journal papers are cited in the report that provide additional information. Many lessons have been learned. Some are not directly transferable to FORGE, but the underpinnings of the lessons may be applicable.

Data processing, annotation, and integration

- A large quantity of new data was managed by the Collab project by data scientists working with subsurface scientists to create a workable data storage and distribution system - the Data Foundry.
- This system allowed easy input of data, and easy access and sharing with others.
- Organizing, annotating, and presenting many streams of data in a readily understood manner *as soon as possible* facilitated better decision-making and data archiving.

Data from many tests and techniques has been collected during Collab Experiment 1 resulting in a large quantity of data (several hundred Tb). At the outset of the Collab project, a data management plan was designed and implemented by data scientists working directly with data generators and data users. Multiple systems were developed to transfer, store, and make available the different kinds of data. These data and systems include management and coordination information on a commercial communication platform (Teamwork), project-relevant data on a commercial cloud system (Google Drive), scientific data of interest to EGS, and subsurface science (the Data Foundry, leading to submittal to the Geothermal Data Repository). The first two of these systems declined in use and were largely replaced by the Data Foundry. This system had an active data scientist who managed and modified the system to meet user needs and to improve its performance and ease of use over time. This system was maintained as the backbone of project data management.

Collab team members are based in many locations, thus the ability to live-stream data in a visual format during active experiments facilitated engaging our team members to make real-time decisions. It is noteworthy to emphasize the importance of organizing, annotating, distributing and presenting many streams of data *as soon as possible* in a readily understood graphic manner. This facilitated making informed engineering decisions, as well as summarized data for future use by prospective data consumers. Making experimental data reachable and understandable to a broader community helped both expand the perspectives to scientific and engineering interpretations as well as make many important discoveries. Temporal and/or spatial synchronization of multi-faceted data sets was found to reveal processes that may be obscured in individual measurements, and/or corroborate other data streams allowing for more definitive conclusions.

Currently in the FORGE project, there is a great deal of drilling data that has been compiled using the RigWatch program. These data provide real-time monitoring of main drilling parameters. These data could be made available to people interested in research drilling mechanics. Stress testing data (i.e. rate and pressure) at FORGE are also of interest to the community - immediately and in the future. Currently, this drilling information is archived by the pumping service company and the company that provides the recording capabilities for drilling, however rapid access to the data by direct archiving should be considered. The many tests planned at FORGE will also generate a large amount of data. If these data are available to researchers, collaborative interpretations will be facilitated.

Processing seismic data

- Application of edge computing to filter high-bandwidth microseismic data resulted in rapid location of microseismic events useful in near-real-time decision making.

- Clear microseismic maps provided excellent spatial (and temporal) constraints on the seismically active fracture planes.
- Machine learning methods were developed to rapidly separate useful data from noise.
- Seismic data streams generated using the fiber optic sensing system (DAS) have required more intensive analysis and interpretation. New approaches are being developed to speed up the use of these data which may be beneficial for DAS use and interpretation at FORGE.

Active and passive seismic data are key subsets of the Collab data. An intensively equipped seismic monitoring system in the Collab Testbed 1 was deployed with a goal of imaging fracturing in the experimental rock volume through detection and location of microseismic events, as well as simultaneously acquiring active seismic time-lapse imaging. A large number of sensors and their deployment in a 3D distribution around the stimulation zone via the 6 monitoring wells enabled rapid, high-quality hypocenter determination with spatial resolution at the sub-meter level. Despite the challenges associated with sensor resonance, the high-sensitivity accelerometer pods allowed for production of an extensive event catalog that was refined by machine learning algorithms. Providing access to the most updated version of this catalog allowed for precise identification of fracture planes, even those in close proximity to each other. In contrast to the diffuse "clouds" often seen in EGS pilots, the clear microseismic maps recovered provide excellent spatial (and temporal) constraints on the seismically active fracture planes. The value of these data was increased by an edge processing framework developed within the Collab project to identify relevant events, which allowed for near real-time event detection and location.

Edge analysis (rapid limited automatic processing of the data) was needed due to the very large data collection rate. Continuous recording at 100 kHz required by the high event frequency exceeded the available data transfer capability. We developed and implemented machine learning algorithms to separate microseismic signals from noise such as rail traffic or triggering of the electrical resistance tomography (ERT) system. This real-time capability provided almost immediate feedback to field operations. Transfer of data to off-site locations was challenging but manageable (physical transfer of hard drives). Seismic data streams from the fiber optic sensing system (DAS) have required more intensive analysis and interpretation, which resulted in significant delays in the utilization of these data. New approaches are under development to speed up the use of these data. Such improvements could be beneficial for use at FORGE.

Collab Experiment 1 had an advantage that may also occur at FORGE at some point – the ability to ground-truth microseismic event locations. Our fractures intersected our monitoring wells, and we were able to detect these intersections with non-seismic techniques (e.g. DTS) with fixed locations. This provided additional confidence in the microseismic locations, as well as an explanation of processes affecting the non-seismic data.

Different challenges in monitoring microseismicity will be encountered at FORGE. Well- and surface-based seismic monitoring at FORGE will not encompass the test region like what was done at Collab, and different noise sources will impact measurements. Continuous measurements may be able to utilize the noise sources however to detect changes in the reservoir. Machine learning algorithms may be useful at FORGE to identify important features in the data.

Connecting geophysics, fractures, and flow systems

- A conceptual discrete fracture model based on timely interpretation of core and borehole observations created a basis for numerical evaluations.
- The model was improved continuously by incorporating inferences from each new data set.
- Repeated sets of measurements showed system changes, complicating interpretation.
- Some Collab monitoring methods will require novel approaches for use at FORGE.

Discrete Fracture Network Model

Reconstruction and orienting core provided critical information on the subsurface environment. Core samples were invaluable in determining simulation parameters for hydrologic, thermal and geologic modeling, often the only source for such parameters. Core samples and wireline logs were also helpful in identifying locations of fracture-borehole intersections, and characterizing those intersections. This task needs to be performed in a timely manner to provide ground-truth information for use in models. Immediate correlation to wireline measurements allows extension of the ground-truth information and more reliable interpretation of the wireline data.

Direct observation of complete cores, interpretation of image logs, and fracture/shear zone mapping in the testbed vicinity were incorporated into a discrete fracture network (DFN) model, which served as a basis for conceptualizing fracture flow pathways. These observations were supplemented by geophysical and hydrologic measurements. For example, passive microseismic, ERT, and tracer tests characterized natural and hydraulic fractures and flows in the testbed. Valuable steps towards interpretating tracer data to predict thermal behavior have been undertaken to address this long-standing issue, however, additional techniques are still required and are being developed. Recently, the Collab team has developed a new approach to predict long-term thermal performance of an EGS system from short-term tracer tests. By drawing an analogue from stochastic history matching in petroleum engineering, we infer flow characteristics on heterogenous fracture networks by assimilating conservative and sorptive tracer data. The inference is non-unique, and we use an ensemble-based stochastic framework to achieve uncertainty quantification.

Despite being able to characterize and monitor major natural and created fractures at individual levels, challenges in disentangling the fracture system's thermal exchange/heat extraction in the testbed exist. The Collab system was dominated by a small number of fractures, and the major flow paths changed from time to time. Numerical simulations of tracer and thermal recovery were able to reproduce the experimental observations using a small number of dominant fractures that were aligned with the seismic event locations.

The FORGE DFN is largely based on formation microimager (FMI) data and outcrop measurements. As with Collab’s, the DFN is regarded as living model and has been continuously updated based on all new data as it became available.

Reservoir Evolution

A multi-pronged interrogation approach was implemented to characterize and monitor reservoir evolution during Experiment 1. The MEQ monitoring system was the primary tool used for imaging the propagation and extent of hydraulic fractures. Additional measurements such as flowrate, pressure, electrical resistance tomography (ERT), distributed fiber optic sensing (temperature -DTS, strain DSS, and acoustic - DAS), downhole camera observations, and tracer testing aided in the interrogation of Experiment 1 as well. This comprehensive monitoring system enabled us to compare the detailed testbed behavior described by the entirety of the data to corresponding inferences about testbed behavior derived from a single type of data. This comparison is useful for placing appropriate expectations, strengths, and caveats on inferences derived from a single data type. For example, tracer tests helped reveal the dynamic behavior of the test bed, where the proportions of flow through different fracture networks varied with time. Other methods were less sensitive to this.

Time-lapse measurements using multiple techniques including simple hydrological to geophysical methods improved the understanding of the initial system, *and* changes in the system. Repeat and similar measurements made at FORGE, should be jointly interpreted when new data become available to identify likely changes in the subsurface system. Adequate emphasis must be placed on processing the collected data. Joint interpretation of multiple data streams is key to providing additional understanding. Rapid sharing of data at FORGE might be difficult because numerous parties will be collecting data. A unified data collection and sharing platform where data must be rapidly posted and shared would help in understanding the FORGE reservoir.

Some Collab successes were related to our capacity to use many highly instrumented dedicated monitoring wells to fully surround the target zone with sensors. For example, this resulted in high accuracy hypocenter determination. This approach also enabled the deployment of relatively new techniques such as continuous active source seismic monitoring (CASSM) and dynamic electrical resistance tomography (ERT) for one of the first times in a complicated geothermal testbed. Consideration of new monitoring technologies such as these under EGS conditions should be considered in the ongoing plans for FORGE. It is recognized that not all the techniques used in Collab are directly implementable at FORGE because of the temperature and cost of application; their use at Collab provides a broader description of processes. The use of multiple modalities of fiber optic sensing (distributed temperature, acoustic, and seismic sensing – DTS, DAS, DSS) has been extremely valuable at Collab for the low relative cost and quality and quantity of data collected. These techniques are likely compatible with the subsurface conditions at FORGE.

Challenges of modeling fractured flow systems

- Simulations were relied upon to guide design of experiments, explain observations, and predict responses to changes in operation.
- Numerous comparisons of data and models provided confidence in the modeling process and the simulators. At FORGE, model-data and model-model comparisons and code improvements should be made available to other researchers by means of a clearinghouse.
- Near-real time simulation was facilitated by the use of high-quality baseline models.
- Model-data comparisons with simulations can be used to identify the measurements needed to distinguish between processes (e.g. poroelastic effects vs. fracture plugging).

A principal objective for the project is learning whether the capabilities of modern state-of-the-art simulators are sufficient to accurately predict stimulation, fracture networks, and subsequently thermal energy recovery for the Collab experiments. In the Collab project numerical simulations 1) supported or refined experimental designs, 2) were used to estimate the magnitudes of the effects of the applied stimuli to obtain approvals to proceed, 3) forecasted outcomes of operational changes, and 4) provided an understanding of observed behaviors.

Factors that built confidence in numerical simulation included 1. modelers starting with a detailed understanding of the experiments, and 2. expert use of codes that incorporate known processes to the extent reasonable. Simulations were performed in near-real-time, and yielded reliable, high-quality solutions. The limitations of the models and simulations were also explicitly stated, so the results could be appropriately valued and used. The key to fast (often overnight) turnarounds of simulations accompanying stimulations was to build high-quality baseline models in the experiment design phase and incorporate new observations and parameters as they became available. To facilitate rapid model building at FORGE with a goal of near real-time analysis, all models created for use on the FORGE project including the grid files should be made available for use by other modelers, perhaps by means of a clearinghouse.

Unknowable heterogeneities are present in the rock fabric, as well as natural fractures, spatial variations of in-situ stress, and other geologic features. These preclude numerical simulation from providing highly spatially accurate matches to experimental outcomes. The true value of numerical simulation comes from the understanding it provides concerning complex system behavior, allowing informed choices to be made about experimental designs and in interpreting empirical observations. Experiment 1 yielded a number experimental observations that at first consideration seemed counter intuitive, such as temperature spikes at intersections between fractures and monitoring boreholes, water production in monitoring boreholes beyond the production borehole, sharp pressure drops after restarting following short injection halts. Because of the number of variables and the complexity of the system, numerical simulations were needed to provide either potential explanations for the observations, or rule out unlikely hypotheses.

Large-scale validation efforts have not been performed in the Collab project comparing simulations and measurements for an entire experiment yielding "approved" validated software packages. Numerous simulations have been performed and compared to measurements. These comparisons provide measures of validation for the conditions modeled. It is implicit here that the simulators, when used by experienced modelers seeking mechanistic explanations, can provide valuable information for planning, interpretation, process quantification, and system understanding. The ability to perform near-real time simulations to provide suggested explanations to observations attests to the confidence in the simulators, and the modeling and simulation *process*. Part of the validation process requires simulators to be improvement when differences between the simulations and measurements occur.

There are many remaining challenges in simulating fracture flow and heat extraction. Understanding the interplay between poroelastic, thermal, chemical, mechanical, and biological processes is thought to be important to interpreting injection-pressure data. The rates at which chemistry may impact flow can be surprisingly fast, complicating injectivity data interpretation. Even with the sophisticated measurement techniques available, it may not be possible to know boundary conditions on the scale that mechanistic models may require. Thus, a disconnect must often be accepted between actual and model boundaries. Reducing the severity of this disconnect may be necessary for determining which process creates the difference between observed and modeled results. When clever models are created to overcome these disconnects, the modeling tools should be collected and made available to other FORGE researchers, perhaps by means of a clearinghouse.

Another challenge is modeling a dynamic system. In Experiment 1, the flow rates at multiple locations changed over time. It is unclear what processes are responsible for those changes and whether these processes are already included in the simulators. Without additional observations and data, one can only speculate on the causes. However, the models can be used to offer insights into processes and process magnitudes, and provide a guide to the next measurements needed to determine the responsible processes. Experiment 1 taught the modeling community that every element in the suite of THMC processes needs to be considered to understand the dynamic and unpredictable nature of EGS reservoirs. Quite often EGS reservoirs are conceptualized as TH systems, which is generally sufficient for design, prototyping, or optimization studies, but truly understanding the more challenging observed behaviors of a particular reservoir will require full coupling of all the processes and full coupling of modeling expertise across these processes.

In Experiment 1, evaluating the ability of the numerical simulation tools to predict thermal recovery was especially challenging for three reasons, 1) the relatively low flow rates, 2) the relatively high thermal conductivity of the matrix rock, and 3) the thermal gradients present in the rock from cooling over a 50-year mining period. Nevertheless, the simulators were able to accurately reproduce the observed nearly constant production temperature over the course of the 196-day chilled-water circulation test. We anticipate commercial-scale applications, such as FORGE, to yield stronger temperature differences and signals for comparisons against simulation tools.

The tests and experiments that will occur at FORGE will result in numerous observations and many of these may be difficult to explain. Identifying processes that could result in these observations will require appropriate models, good simulators, and knowledgeable modelers willing to consider all possible solutions. Applying simulation tools used in Collab to FORGE or other projects with elevated temperatures will require stepwise confidence-building in the hands of experienced modelers knowledgeable of the processes occurring. If this is performed, the process is likely to be successful. Specifically, thermomechanical, poroelastic, and geochemical changes will occur at different rates than at Collab. Higher temperature will strongly affect geochemistry including dissolution and precipitation. Temperature gradients are likely to be much higher at FORGE, more strongly affecting thermomechanical behavior. Rock properties may also vary over the strong gradient, and the ability to simulate *all* of these processes will be needed. An advantage at FORGE is the ability to drive the system harder and over a larger range of flows and temperatures than at Collab. These factors will be helpful in determining the relative contribution of processes to the observed behavior.

Acknowledgements

This material was based upon work supported by the U.S. Department of Energy, Office of Energy Efficiency and Renewable Energy (EERE), Office of Technology Development, Geothermal Technologies Office, under Award Numbers DE-AC02-05CH11231 with LBNL, DE-AC07-05ID14517 with INL, DE-AC05-76RL01830 with PNNL, DE-AC52-07NA27344 with LLNL, DE-NA0003525 with SNL, 89233218CNA000001with LANL, DE-ACO5-000R22725 with ORNL, and DE-AC36-08GO28308 with NREL. The research supporting this work took place in whole or in part at the Sanford Underground Research Facility in Lead, South Dakota. The assistance of the Sanford Underground Research Facility and its personnel in providing physical access and general logistical and technical support is gratefully acknowledged. The earth model output was generated using Leapfrog Software. Copyright © Seequent Limited. Leapfrog and all other Seequent Limited product or service names are registered trademarks or trademarks of Seequent Limited. The common discrete fracture network model of the testbed was created using FracMan software (Golder Associates, Inc.).

Abbreviations and Symbols

CASSM	:	Continuous Active Source Seismic Monitoring
C-dot	:	Carbon-dot
CSM	:	Colorado School of Mines
CSV	:	Comma Separated Value
DAS	:	Distributed Acoustic Sensor
DEM	:	Discrete Element Model
DFN	:	Discrete Fracture Network
DNA	:	Deoxyribose Nucleic Acid
DOE	:	Department of Energy
DSS	:	Distributed Strain Sensor
DTS	:	Distributed Temperature Sensor
DUSEL	:	Deep Underground Science and Engineering Laboratory
E1-I	:	Experiment 1- Injection hole
E1-P	:	Experiment 1- Production hole
E1-PDB	:	Experiment 1- Parallel Deep Bottom monitoring hole
E1-PDT	:	Experiment 1- Parallel Deep Top monitoring hole
E1-PSB	:	Experiment 1- Parallel Shallow Bottom monitoring hole
E1-PST	:	Experiment 1- Parallel Shallow Top monitoring hole
E1-OB	:	Experiment 1- Orthogonal Bottom monitoring hole
E1-OT	:	Experiment 1- Orthogonal Top monitoring hole
EC	:	Electrical Conductivity
EGS	:	Enhanced Geothermal Systems
ERT	:	Electrical Resistance Tomography
FORGE	:	Frontier Observatory for Research in Geothermal Energy
GDR	:	Geothermal Data Repository
GTO	:	Geothermal Technologies Office
INL	:	Idaho National Laboratory
kISMET	:	Permeability (k) and Induced Seismicity Management for Energy Technologies
LANL	:	Los Alamos National Laboratory
LBNL	:	Lawrence Berkeley National Laboratory
LLNL	:	Lawrence Livermore National Laboratory
MB		Mega Bits
MEQ	:	Micro Earthquake
NREL	:	National Renewable Energy Laboratory
PB	:	Production hole Below lower packer
PI	:	Production hole Interval
PNNL	:	Pacific Northwest National Laboratory
PVC	:	Polyvinyl Chloride
ORNL	:	Oak Ridge National Laboratory
SDSTA	:	South Dakota Science and Technology Authority
SIMFIP	:	Step-rate Injection Method for Fracture In-situ Properties
SNL	:	Sandia National Laboratory
SURF	:	Sanford Underground Research Facility

THMC	:	Thermal-Hydrological-Mechanical-Chemical
VTK		Visualization Toolkit
cm	:	Centimeter
º C	:	Degree Celsius
k	:	Permeability
kHz	:	Kilo Hertz
kJ	:	Kilo Joule
kPa	:	Kilo Pascal
L	:	Liter
m	:	Meter
mL	:	Milliliter
mm		Millimeter
MPa	:	Mega Pascal
Pa	:	Pascal
P	:	Pressure
s	:	Second
σ_h, σ_H, σ_v	:	Minimum horizontal stress, maximum horizontal stress, vertical stress
T	:	Temperature
Vp	:	Compressional wave velocity
Vs	:	Shear wave velocity

1. Introduction

This report describes a subset of learnings from the EGS Collab (Collab) project (https://openei.org/wiki/EGS_Collab_Project_Overview) to date that may be applicable to the Frontier Observatory for Research in Geothermal Energy (FORGE) project (https://utahforge.com/). We focus on learnings of the Collab within topic areas requested by FORGE. Learnings, recommendations, and insight included in this report are based on the results, observations, and perspectives of Collab scientists following the completion of Collab Experiment 1.

1.1 Topics in this report

Several topics are discussed in this report. These topics were identified by FORGE as important and include:

- Data processing, annotation, and integration
- Seismic data processing
- Connecting geophysics, fractures, and flow systems
- Challenges of modeling fractured flow systems

Data processing, annotation, and integration - A large quantity of data was gathered in the Collab. Data generated from the Collab monitoring systems have been used for two main purposes: 1) engineering decision making, and 2) scientific interpretation of observed phenomena. To be useful for decision making, data had to be rapidly interpreted to the extent needed for the decisions, and presented graphically as soon as possible. Several data streams were processed this way, with more refined scientific analyses following the engineering decisions. In many cases, the subsequent analyses led to improvements in the rapid processing, yielding in better results for decision making (Section 2).

Seismic data processing - The dynamic nature of fracture behavior required development of rapid analysis methods. The Collab micro-earthquake (MEQ) data collection rate exceeded the data transfer rate to external computers for the complex processing. This led us to make some simplifications, such as 1) filter data to identify events of interest, 2) rapidly process and locate the MEQs using an onsite computer, and 3) display and broadcast the hypocenters for near-real time decision making. Subsequent detailed evaluation of the data led to better rapid analysis methods (Section 3).

Connecting geophysics, fractures, and flow systems - Besides MEQs, additional monitoring techniques were also deployed in the testbed. Electrical resistance tomography (ERT), distributed fiber optic sensing, and continuous active source seismic monitoring (CASSM) along with multiple tracer tests were used to identify fractures and flow systems (Section 4). Disparate data sets were validated by results from overlapping techniques. In addition, the geologic/borehole characterization data integrated with geophysical and tracer data were crucial to locate and image fractures that hit production and monitoring wells and validate MEQ locations (Section 5).

Challenges of modeling fractured flow systems - Numerical simulations, which are essential to the project mission, were initially used to help design the mesoscale experiments and forecast outcomes of processes. Following completion of tests and subtests, the experimental datasets were used to validate and refine numerical models making them more applicable and relevant to FORGE and EGS (Section 6). Detailed simulations have also been used to interpret data, understand observations, and identify and rule out processes.

We provide a brief description of both projects with sufficient detail to allow a reader to understand the similarities and differences between the projects and provide information aiding in interpreting and extending the learnings of Collab to FORGE.

1.2 The EGS Collab Project

To facilitate the success of FORGE and EGS, the US Department of Energy (DOE) Geothermal Technologies Office (GTO) initiated the EGS Collab project. Collab is utilizing readily accessible underground facilities to refine understanding of rock mass response to stimulation using ~ 10 m scale (intermediate scale) experiments under EGS-relevant stress conditions. The primary objective of this project is to conduct a series of experiments and use the experimental results to validate coupled thermal-hydrological-mechanical-chemical (THMC) modeling approaches applicable to EGS. Collab is also testing and improving conventional and novel field monitoring tools. Collab focuses on understanding and predicting permeability enhancement and evolution in crystalline rock, including how to create sustained and distributed permeability for heat extraction from a reservoir by generating new fractures that complement existing fractures. It is a collaborative multi-national-lab, university, and commercial entity research endeavor bringing together a team of skilled and experienced subsurface process modeling, monitoring, and experimentation researchers and engineers to focus on intermediate-scale EGS reservoir creation processes and related model validation in crystalline rock (Kneafsey et al., 2018; 2019a,b; 2020a,b).

The project is embodied in three experiments planned to increase understanding of 1) hydraulic fracturing (Experiment 1- completed), 2) shear stimulation (Experiment 2 – test bed construction underway), and 3) other stimulation methods in Experiment 3. Each experiment begins with modeling to support experiment design and consists of a series of tests. Post-test modeling and analysis are performed to examine the effectiveness of our modeling tools and approaches.

In Experiment 1, we performed several highly monitored hydraulic fracture stimulations and flow tests, and implemented a suite of rock/reservoir characterization methods potentially useful for EGS, as well as other methods available to improve system understanding (Knox et al., 2017; Morris, et al., 2018). The monitoring/characterization methods (Table 1.1) are intended to help define the geometry of the propagated fracture(s), constrain the effective heat transfer surface area in the reservoir, and determine the flow rate limitations for sustaining production well temperatures (Doe et al., 2014; Zhou et al., 2018). One key component of the project is thermal circulation tests that will be used to validate predictions based on field data and stimulations.

This report will not detail all aspects of Collab Experiment 1. Numerous conference and journal publications are available containing testbed design, tests, observations, and detailed analyses (https://scholar.google.com/citations?hl=en&user=h-rd4hkAAAAJ). In addition, project data are available from the DOE's Geothermal Data Repository (GDR, https://gdr.openei.org/egs_collab).

1.2.1 Site description - Testbed 1

Testbed 1 on the 4850 (feet deep) level at the Sanford Underground Research Facility (SURF, Figure 1.1) in Lead, South Dakota (Heise, 2015) was used to conduct Collab Experiment 1. SURF is operated by the South Dakota Science and Technology Authority (SDSTA) and occupies the former Homestake gold mine. As a former gold mine and current underground laboratory, SURF has been very well characterized in some ways (e.g., Hart et al., 2014), and provides infrastructure (e.g., ventilation, power, water and internet) and research support staff, in addition to cost-effective proximal monitoring of a deep crystalline rock mass before, during, and after stimulation through multiple boreholes drilled from an underground tunnel. This enables performing tests under realistic *in situ* EGS stress conditions (Dobson et al., 2017). The maximum rock temperature at the 4850 level is about 35°C, which is not optimal for a geothermal project. However, achieving realistic temperatures *and* stress would involve costly deep drilling and would not facilitate detailed characterization and monitoring, and would have prevented achieving the Collab objectives.

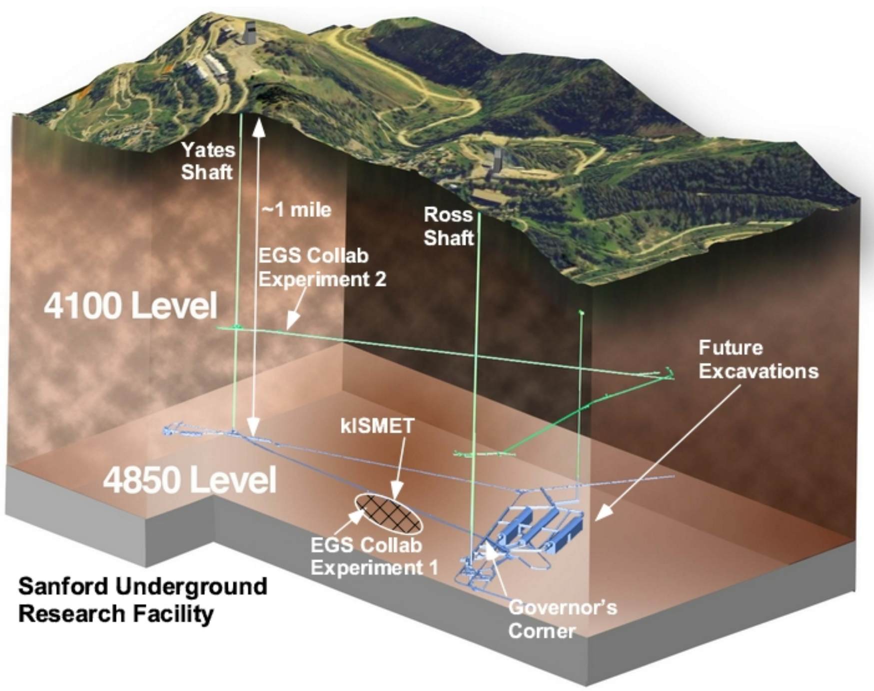

Figure 1.1: Schematic view of the Sanford Underground Research Facility (SURF), depicting a small fraction of the underground facilities including the Yates & Ross shafts, 4850 level & 4100 level, and Testbed locations of the kISMET, Collab Experiment 1, & Collab Experiment 2.

Experiment 1 was intended to establish a fracture network that connects an injection well and a production well using hydraulic fracturing (Morris et al., 2018). A schematic of the Experiment 1 testbed (Testbed 1) is shown in Figure 1.2. All boreholes for the experiment are nominally 60 meters long, drilled subhorizontally, and were continuously cored. The injection and production boreholes were drilled in approximately the minimum principal stress direction based on prior characterizations at nearby Permeability (k) and Induced Seismicity Management for Energy Technologies (kISMET) testbed (Oldenburg et al., 2017) so that hydraulic fractures were expected to propagate orthogonally to the injection well. Six monitoring wells were drilled, and instrumentation (Table 1.1) was grouted in these wells.

Table 1.1: Testbed 1 characterization and monitoring tools and techniques

Borehole characterization • Optical and acoustic televiewers • Full waveform sonic • Electrical resistivity • Natural gamma • Temperature/conductivity logs
Test block characterization • Compressional- and shear-wave seismic tomography using grouted and mobile sources and sensors (Linneman et al., 2018; Morris et al., 2018; Schwering et al., 2018) • Electrical resistance tomography (ERT) for baseline and during flow (Johnson et al., 2019) • Extended hydrologic characterization including tracer tests (Mattson et al., 2019; Neupane et al., 2020; Mattson et al., 2021) • Stimulation and flow test monitoring and analysis • Passive seismic monitoring (Chen et al., 2018; Huang et al., 2017; Newman and Petrov, 2018; Schoenball et al., 2019; Fu et al., 2021) • Continuous Active Source Seismic Monitoring (CASSM) (Gao et al., 2018) • ERT in conjunction with dynamic electrical imaging using high contrast fluids (Johnson et al., 2014; Johnson et al., 2019; Wu et al., 2018) • Acoustic emissions (e.g. Zang et al., 2017) • Distributed fiber optic sensors to monitor changes in seismicity (distributed acoustic sensor, DAS), temperature (distributed temperature sensor, DTS), and strain (distributed strain sensor, DSS) (Fu et al., 2021) • Step-rate Injection Method for Fracture In-situ Properties (SIMFIP) tool (Guglielmi et al., 2013; Guglielmi et al., 2014; Guglielmi et al., 2015; Guglielmi et al., 2021) • Continuous monitoring of pressure and flow conditions in the injection and production boreholes (Fu et al., 2021) • Tracer tests (Zhou et al., 2018; Mattson et al., 2019, Neupane et al., 2020, Mattson et al., 2021; Wu et al., 2021) • Wavefield imaging and inversion (Chen et al., 2019; Gao et al., 2018; Huang et al., 2017; Knox et al., 2016; Newman and Petrov, 2018)
Geophysical monitoring equipment installed • Seismic sensors (hydrophones and accelerometers) • Seismic sources and receivers for CASSM • ERT electrodes • Fiber for distributed strain, acoustic, and temperature sensing • Thermistors

1.2.2 Baseline fracture network

Testbed 1 (Figure 1.2) was developed in the Precambrian Poorman Formation containing graphitic sericite-biotite phyllite/schist with local interlayers of quartz and calcite veins. Regionally, the testbed is located on the west limb of the plunging Lead anticline structure. Locally, rocks in the testbed show intense folding with small crenulations to meso-scale folds with a series of sheared/weak zones and two sets of dominant natural fractures.

Initially, it was expected that Testbed 1 would have very little hydraulic connectivity between boreholes or to drift because of the presence of limited natural fractures in the vertical boreholes at the nearby kISMET testbed (Oldenburg et al., 2017; Dobson et al., 2017) and the sparsity of flowing fractures in the boreholes that were drilled for Deep Underground Science and Engineering Laboratory (DUSEL) in 2009 (Carter et al., 2011; Roggenthen, 2013). However, the discovery of borehole crossflows led to a series of flow tests by pressurizing one borehole and observing outflows in the other boreholes using a downhole television camera. These fractures were sufficiently conductive to influence the experiment, but poorly connected to groundwater sources so they did not flow continuously under natural conditions.

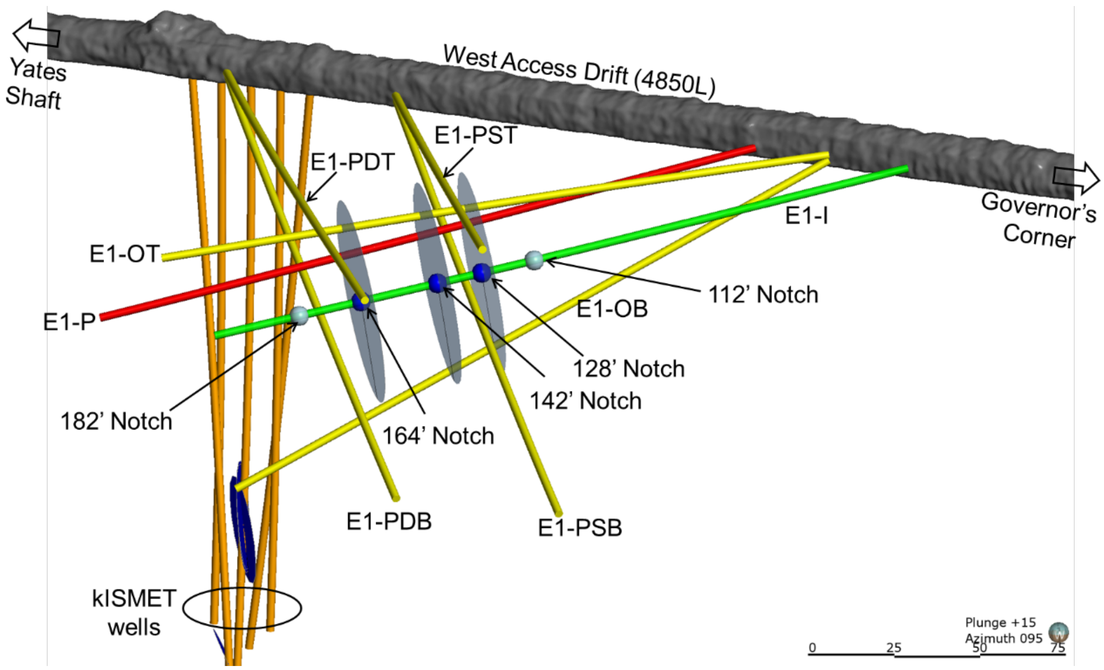

Figure 1.2: Schematic of wells in the Testbed 1 along the West Drift on the 4850 level of SURF. The green line represents the stimulation (Injection) well (E1-I), the red line represents the Production well (E1-P), yellow lines represent monitoring wells, and orange lines represent kISMET wells. Orientation of stimulation and production boreholes is approximately parallel to S_{hmin} and the gray disks indicate nominal ideal hydraulic fractures.

The baseline discrete fracture network (DFN) model (Figure 1.3) of the testbed was developed by identifying the specific conducting fractures in each hole and their likely intersections in other holes using flow data from the boreholes, optical and acoustic televiewer data, inspection of cores with fractures, and seepage mapping along the nearby drift walls (Roggenthen et al., 2018; Ulrich et al., 2018; Schwering et al., 2020). The DFN has been continuously updated as new became available.

In general, the acoustic image logs proved to be the most useful for defining the existing fractures in the testbed because they yielded the greatest contrast and were not affected by water clarity. The optical televiewer was useful for imaging bedding features and, in many instances, healed fractures when the water was sufficiently clear. Moreover, intensely deployed and continuously monitored geophysical tools helped refine the baseline fracture model as well as capture the evolving nature of the fracture systems in the testbed. Specifically, data such as 1) temperature anomalies picked at different depths along the boreholes by DTS, 2) distribution of MEQ hypocenters during stimulation and flow tests, 3) time-lapse ERT along with outflow patterns from production/monitoring holes, and 4) tracer breakthrough data for various producers provided important data for imaging/monitoring permeability enhancement and evolution at the reservoir scale to the resolution of individual created fractures (Schoenball et al., 2019a; Johnson et al., 2019; Neupane et al., 2019; Mattson et al., 2019; Wu et al., 2021; Fu et al., 2021).

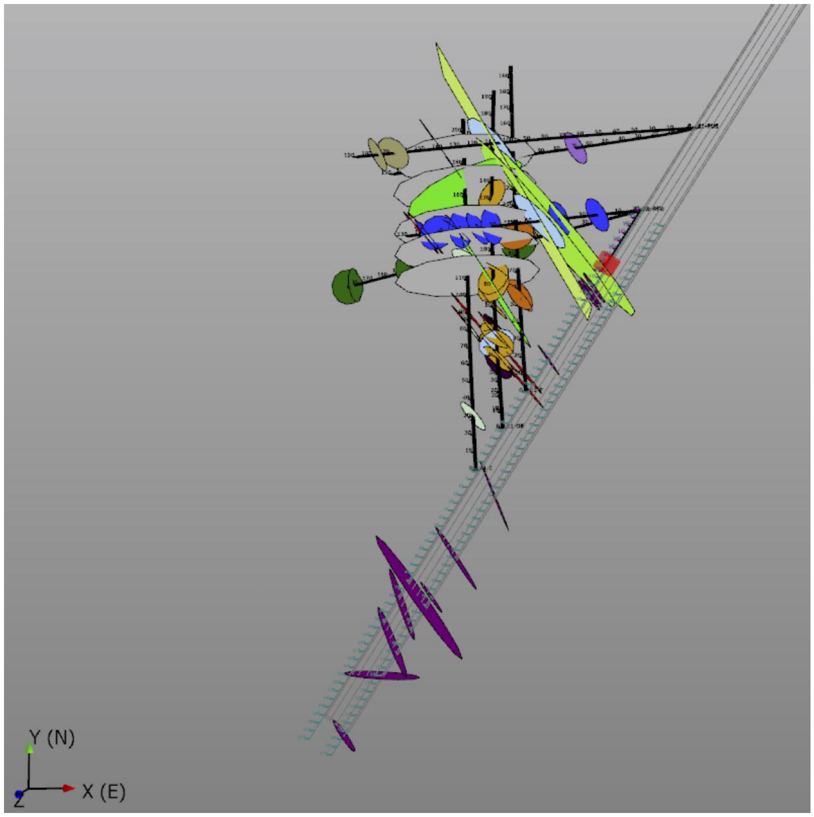

Figure 1.3: Common discrete fracture network of Experiment 1.

1.2.3 Laboratory measurements

Laboratory tests on selected core samples from the site were conducted to measure fundamental physical rock properties needed to constrain the coupled process models. In addition, a complementing suite of data from kISMET (Oldenburg et al., 2017; Wang et al., 2017) and previous geotechnical studies at SURF were also used in our modeling efforts. Laboratory investigations have also been undertaken to provide additional system understanding (Condon et al., 2020) and process understanding (Frash et al., 2018a; Frash et al., 2018b; Yildirim et al., 2018; Frash et al., 2019; Ye et al., 2019; Meng et al., 2021, Li et al., 2021).

1.2.4 Stimulations performed

Summaries of stimulations, long and short-term flow tests, and tracer tests have been presented elsewhere (e.g., Kneafsey et al., 2020a; Kneafsey et al., 2019a; Mattson et al., 2019; Neupane et al., 2020; White et al., 2019) and will not be described in detail here. Briefly, notches were scribed at specified locations along the injection well to encourage perpendicular fracturing (Section 6.1.3). The stimulations were planned to occur in 3 steps. The first step was intended to create a 1.5 m radius penny-shaped fracture prior to being shut in for the night. The second step would extend the fracture to 5 m radius followed by being shut in for the night, and the third step would extend the fracture to the production borehole approximately 10 m away. Briefly, four stimulation tests and short- and long-term ambient temperature and chilled water flow tests were performed, resulting in many data sets and analyses (see references in Kneafsey et al., 2020a).

1.2.5 Flow tests

Long-term ambient temperature and chilled water flow tests were performed for about 10 months in Experiment 1. In these tests, water was introduced at the 164' Notch interval, typically at 0.4 L/m. This rate, although lower than desired, did not result in additional microseismicity, indicating that the stimulated system was seismically stable, and the fracture network was stable. Volumetric recovery of the injected water increased over the duration of the test reaching near full recovery from combined collection points, however, not all from the production well. In spite of reaching high volumetric recovery, tracer and microbial analyses (Mattson et al., 2019; Zhang et al., 2020) indicate that the recovered water has differences from the injected water, indicating perhaps that the injected water is displacing and mixing with native water in the system, or the water is altered in different manners along several flow paths.

1.3 FORGE

FORGE is the major EGS initiative of GTO with the mission of establishing a site that enables cutting-edge research and testing for drilling and EGS technology as well as allowing scientists to identify a replicable, commercial pathway to EGS. GTO initiated the FORGE effort in 2014 with the selection of five first-phase projects. After the first and second phase downselect processes, the Utah FORGE was selected to create a full-fledged EGS test site in 2018. Some of the salient features of the FORGE and Collab are given in Table 1.2.

Table 1.2: Salient features of Collab and FORGE

Attributes	Collab	FORGE
Scale	Intermediate (~10 m)	Full reservoir
Temperature	Low (20-35º C)	EGS (175-225º C)
Stress/Depth	1.25 – 1.5 km	1.8-2.5 km
Focus	Examine/quantify/simulate stimulations and permeability enhancement	Independent multiparty investigations at EGS field laboratory
Research Program	Collaborative test performance and evaluation	Establish EGS field laboratory, and perform tests, manage funded research program
Rock Access	Short narrow boreholes from mine tunnels	Deep wells from surface

FORGE, led by the University of Utah, will capture, adapt, and utilize recent drilling and hydraulic stimulation technological advances employed by the oil and gas industry to geothermal systems, on a path to enable geothermal energy to realize its potential as a widespread source of renewable power. These advances will initially be realized in well drilling, well completion, and reservoir stimulation methods. The goal of the FORGE is to demonstrate to the public, stakeholders, and the energy industry that EGS technologies have the potential to contribute significantly to future power generation (Moore et al., 2019).

1.3.1 Site description

The FORGE site is located near the town of Milford in south-central Utah (Figure 1.4A). The FORGE footprint covers an area of about 5 km^2 adjacent to PacifiCorp Energy's 38 MWe Blundell geothermal plant at Roosevelt Hot Springs. Geologically, the site is located on the eastern edge of the Milford basin, west of the Minerals Mountains (Figure 1.4B-C). The geology of the central Mineral Mountains is dominated by a composite Tertiary pluton composed of diorite, granodiorite, quartz monzonite, syenite, and granite (Nielson et al., 1986). The Tertiary pluton is collectively referred to as granitoid, and it will host the FORGE experiments (Figure 1.4D). From the Minerals Mountains, the contact between granitoid and valley fill sediments dips to the west. This site has already undergone significant characterization and testing with collection of a suite of data on fracture orientations, subsurface stress gradients, permeabilities, temperatures, rock types, and fracture distributions. A test well (58-32), was drilled to a depth of 2297 meters, where the maximum temperature of ~200°C was measured at the bottom of the hole (Moore et al. 2019, https://gdr.openei.org/forge).

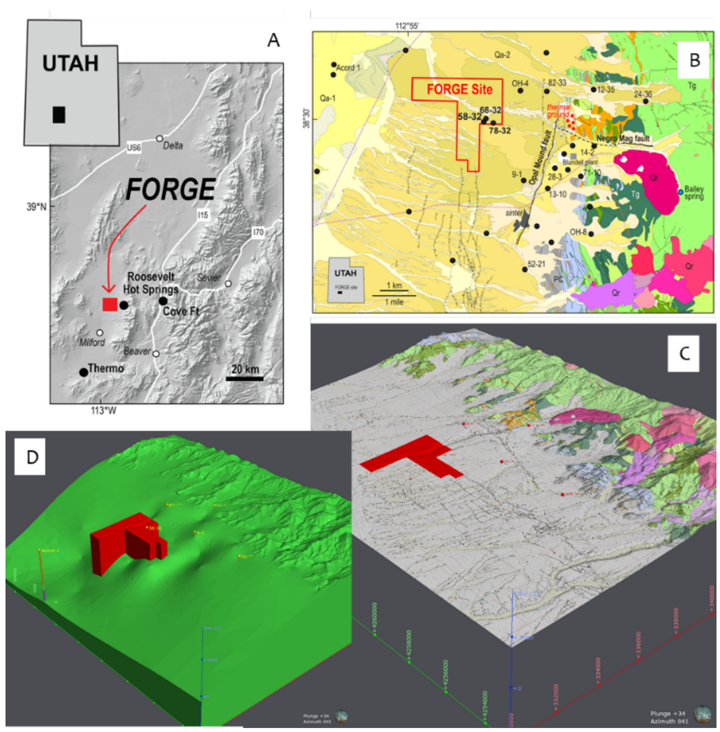

Figure 1.4: A) Location of the FORGE site. B) Surface geology, FORGE site footprint, and key wells (black filled circles) in the area (Moore et al., 2019). C) 3-D geologic model with surface geology and topography. D) 3-D model showing granitoid underneath the valley-fill sediment layers. The FORGE experiments will be performed in the granitoid (red block).

FORGE is currently being developed as a field laboratory to function as a dedicated site for technical interaction and public education to support the widespread adoption of EGS as renewable energy sources. The site had its first EGS-scale, deviated injection well completed early in 2021. This well is expected to undergo partial stimulation, and based on the trend of created fractures, a second well will be drilled in 2022 to intercept those created fractures. With additional stimulations, hydraulic connections between these two well will be established. To better understand and characterize this engineered reservoir, injection and production flow rates and pressures, microseismic events, electromagnetic, geochemical, and tracer data will be accumulated. The monitoring and characterization tools will be used to observe the effects of the stimulation, growth of the stimulated volume with time, fracture interconnectivity, and efficiency of the heat sweep of the created reservoir.

1.4 Collab: Path to FORGE

Although FORGE is being developed as a heavily instrumented full-scale EGS laboratory, the depth below the surface and high temperature within the expected reservoir will limit the ability to closely observe many processes and incidents. The high cost and limitations of access inherent to deep reservoirs place severe limits on our ability to observe fundamental processes critical to EGS development such as fracture creation and sustainable fluid flow for heat extraction. The success of FORGE is expected to be increased by Collab conducting research and development activities and testing in easily accessible underground facilities at meso-scales to refine our understanding of rock-mass response to stimulation and provide a testbed for the validation of THMC modeling approaches as well as novel monitoring tools.

1.5 Interactions between Collab and FORGE

Collab and FORGE are separate DOE-funded projects yet share a common ultimate goal of making EGS a successful technology as a reliable resource of renewable power. There are many collaborators working on both FORGE and Collab projects thus there are many existing avenues for communication of findings external to this report. Collab science, modeling, and field meetings are open, and anyone can attend. Several collaborators on both the Collab and FORGE projects routinely attend Collab meetings and are active members of the Collab project. In addition, the Collab Executive Committee was designed to have representation from FORGE, and those meetings are routinely attended by at least one member of the FORGE team.

2. Data Processing, Annotation, and Integration

Abstract

A large quantity of data has been generated during Collab Experiment 1. Managing and disseminating of data internally within the Collab team as well as among the broader EGS community was conducted by group of data scientists and subsurface scientists through the Data Foundry data storage and distribution system. It is noteworthy to emphasize the importance of organizing, annotating, and presenting many streams of data in an easily understood manner for making informed engineering decisions as well as for future use by prospective data consumers. Making experimental data reachable and accessible to a broader community helped both expand the perspectives to the interpretations as well as make many important discoveries. Individual data sets were validated by results from multiple techniques. Moreover, temporal and/or spatial synchronization of multi-pronged data sets was found to reveal processes that are obscured in individual measurement and/or corroborate each other to draw more definitive conclusions.

2.1 Documentation, Record Keeping, and Data Sharing

The Collab team has diligently and thoroughly documented all activities, incidents, and observations that occurred in the field or in the concurrent tele-meeting supporting field crew during field tests are being carried out. A few practices that the Collab team found valuable are:

a) **Details in daily shift reports.** Common contents of daily shift reports include field work personnel, plans for the day, observations and anomalies, simple direct measurements and sensor calibration results, scanned notes, as well as work photos.

b) **Notes embedded in time-series data.** The flow-and-stimulation system deployed in Testbed 1 recorded more than 90 channels of time-series data from various sensors. Along with these data channels, the operator of the system could type and embed short notes in real time and stream/store these notes in the same comma-separated value (CSV) file along with other data. Figure 2.1 shows the beginning segment of a data file. The notes can be seen in the last column of the data informally named as "metadata". Often trivial-looking incidents happen while experiment is being in progress, and having a record of those incidents and observations with real timestamps helped correlate and interpret measurements observed in other time-series data streams with related events.

c) **Managing and tracking discussions.** Once the Collab team realized the challenge of tracking technical discussions occurring over emails, the team adopted Teamwork (teamwork.com) platform to house all discussions. This proved to be highly effective and served as a form of permanent record.

2.1.1 Centralized, Near-Real Time Sharing of Data

An organized and self-explanatory directory structure, established on OpenEI (https://foundry.openei.org), was used to share, upload, and store data as soon as the data became available (only exception being large-size raw seismic data). In addition, stimulation and flow data were streamed to OpenEI in real time for timely analyses and decision making by a team observing the tests online. Eventually, data files are directly submitted to GDR from Data Foundry for public dissemination (Weers and Huggins, 2019). Data from the OpenEI database are available to all project personnel, and other interested parties.

```
05/22/2018 13:35:10
Time,Quizix Pressure,Quizix Flow,Quizix Cum Vol,Triplex Net Flow,S
hh:mm:ss,psi,LPM,L,LPM,LPM,LPM,LPM,LPM,SLPM,LPM,SLPM,rpm,LPM,psig,
05/21/18 21:31:03,-0.500000,0.000000,1.438279,-0.054287,0.008623,0
05/21/18 21:31:04,-0.600000,0.000000,1.438279,-0.060088,0.008565,0
05/21/18 21:31:05,-0.600000,0.000000,1.438279,-0.026589,0.008876,0
05/21/18 21:31:06,-0.600000,0.000000,1.438279,-0.041396,0.008609,0
05/21/18 21:31:07,-0.700000,0.000000,1.438279,-0.055663,0.011261,0
05/21/18 21:31:08,-0.500000,0.000000,1.438279,-0.044492,0.020696,0
05/21/18 21:31:09,-0.500000,0.000000,1.438279,-0.035918,0.014683,0
05/21/18 21:31:10,-0.600000,0.000000,1.438279,-0.027817,0.011678,0
05/21/18 21:31:11,-0.500000,0.000000,1.438279,-0.021672,0.003321,0
05/21/18 21:31:12,-0.600000,0.000000,1.438279,-0.035147,0.002328,0
05/21/18 21:31:13,-0.500000,0.000000,1.438279,-0.003577,0.017029,0
05/21/18 21:31:14,-0.500000,0.000000,1.438279,-0.031521,0.008583,0
05/21/18 21:31:15,-0.700000,0.000000,1.438279,-0.041261,0.003512,0
05/21/18 21:31:16,-0.600000,0.000000,1.438279,-0.051421,0.014262,0
05/21/18 21:31:17,-0.400000,0.000000,1.438279,-0.045545,0.010571,0
05/21/18 21:31:18,-0.500000,0.000000,1.438279,-0.027400,0.003407,0
05/21/18 21:31:19,-0.500000,0.000000,1.438279,-0.044006,0.008594,0
05/21/18 21:31:20,-0.600000,0.000000,1.438279,-0.046212,0.002690,0...
```

```
ressure,ISCO 3 Tot Vol,PED I TOP,PED I BOT,PED P TOP,PED P BOT,Air P,meta data

00,44.488758,27.790964,-26.305497,-16.503513,96.493507,
00,45.020491,25.873840,-26.964754,-16.762823,96.538918,
00,43.143690,26.783556,-26.458263,-16.764462,96.572576,Prepare for the first stimulation experiment targeting
00,44.048816,25.684029,-27.150303,-15.353501,96.604763,
0,43.749511,25.627315,-27.238160,-14.905363,96.641140,
0,46.319336,28.760999,-28.342605,-15.873760,96.668819,
,45.261443,29.748738,-25.895715,-13.805509,96.700037,
000,44.107169,27.034014,-25.914401,-17.210633,96.712144,
0,44.825107,27.707696,-24.302155,-16.281903,96.738780,
000,43.990463,28.520375,-25.811136,-15.856713,96.767502,
00,43.368578,29.217988,-27.753174,-15.910476,96.783521,
00,44.765770,28.799027,-27.809888,-14.141202,96.796243,
0,44.118643,29.905766,-27.494848,-13.319671,96.819507,
00,43.217450,28.925896,-27.590245,-15.034527,96.825952,
0,44.818550,25.581747,-24.855196,-16.675949,96.844131,
00,45.547307,27.657866,-25.529206,-16.602516,96.866576,
00,45.129001,27.703434,-27.238816,-16.189456,96.874623,
000,43.181390,28.657079,-28.039694,-15.395463,96.885426,
```

Figure 2.1: A truncated snapshot of one of the stimulation and flow time history files (CSV format). The notes (in-file metadata) can be seen in the last column.

2.1.2 Prompt Data and Result Sharing

Collab experiments were planned and carried out iteratively. On each field-work day, the crew (Figure 2.2A) started the work according to a predetermined plan, but the plan was frequently adjusted based on observations. Very often, the daily plan itself had a decision tree built in with many "if" conditions. It is therefore critical to share the data as early as possible to allow informed decisions to steer the experiments to achieve the optimal results.

During each day of testing, six channels (out of 90+) that were most relevant to the objective of the day were displayed on the screen of the data acquisition computer and shared live with all remote participants (Figure 2.2B). A near-real time (within one to two minutes) edge computing microseismic inversion capability played a crucial role in real-time decision-making during experiments as well as for planning the subsequent experiments.

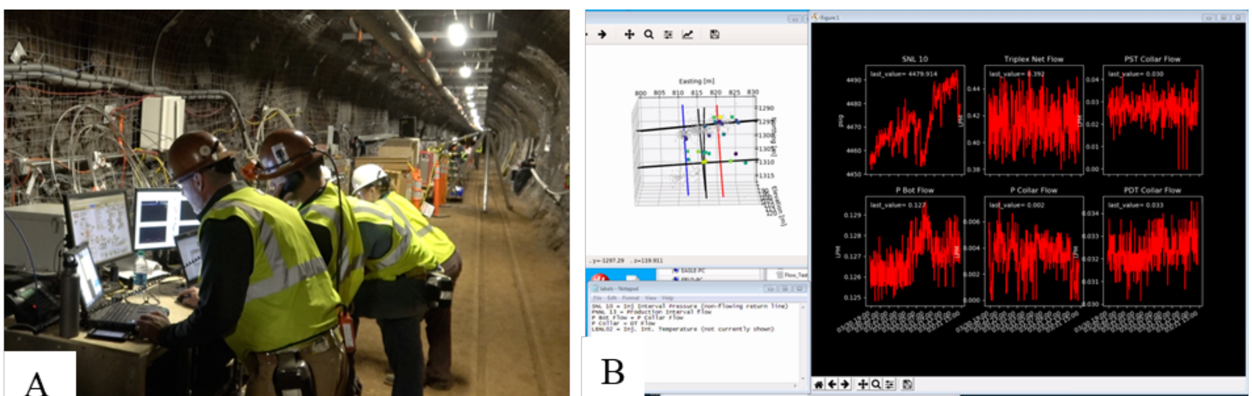

Figure 2.2: Real-time time sharing through an online video conference system. A) Field operation team at the SURF 4850 level. B) Shared screen from the data acquisition computer, with the six dark panels showing time histories in a 24-hour time window. The upper left corner of shared screen shows microseismic events, resolved in near-real time.

2.1.3 Lessons for FORGE

Data practices executed in Collab are very much in line with standard experiment documentation procedures. Because Collab is a centralized project, these practices were largely carried out. However, establishing similar procedures across FORGE may prove more difficult because of the decentralized structure. Currently in the FORGE project, there is a great deal of drilling data that has been compiled using the RigWatch program. These data provide real-time monitoring of main drilling parameters. These data could be made available to people interested in research drilling mechanics. Stress testing data (i.e. rate and pressure) at FORGE are also of interest to the community - immediately and in the future. Currently, this drilling information is archived by the pumping service company and the company that provides the recording capabilities for drilling, however rapid access to the data by direct archiving should be considered. We also note here that as in Collab, FORGE has initiated implementation of data storage and distribution among collaborators using Data Foundry on OpenEI. With the many tests planned for FORGE by various research groups, a large amount of data will soon be created. The integration of Data Foundry as a common platform to store and share data by all research groups would greatly facilitate data accessibility to researchers for collaborative interpretations.

2.4 Synchronization of Multi-source Data

When different measurements are synchronized spatially and/or temporally, they may reveal processes that are not revealed by an individual measurement, or the measurements may corroborate each other to result in more definitive conclusions. Figure 2.3 (see Figure 4.1A for another example) illustrates synchronized injection data, microseismic events, and temperature data by DTS in two wells for a hydraulic test conducted in the Fall 2018. In this plot, it is both noticeable that the injection at higher rates (0.8 to 5 L/minas noted by green arrows “a” through “l” in the upper panel; baseline rate was 0.4 L/min) created MEQs and are detectable in the DTS plots pinpointing where the created/stimulated fractures intersected the wells.

Another example, illustrated in Figure 2.4, shows DTS data measured along the monitoring holes during the first five months of the long-term circulation test in 2019. In addition to the horizontal thin warmer bands that show intersections between flowing fractures and wellbores (indicated by markers “1”, “2”, and “3” in Figure 2.4), wider bands of cooling signals gradually emerged in the E1-PST and E1-PSB (indicated by markers “4” and “5”, respectively) as the result of the injection of cool water. Such wider cooler temperature anomalies also emerged along E1-OT and E1-OB (indicated by markers “6” and “7”, respectively). In a complementary figure (Figure 2.5), the change in temperature from baseline temperature in the monitoring wells is shown at their actual spatial locations. Although the cooling segment in E1-PST seems to coincide with some logged fractures, there are no flowing fractures near the cooling segment in E1-PSB. In addition, the overall cooling in these four affected wells was correlated with the first 50 m of the E1-I which was used for chilled-water circulation. Because of this synchronization of multiple data streams, we hypothesized that the cooling in these four wells was induced by thermal conduction from E1-I. Subsequent modeling work validated that radial conductive cooling did happen, and suggested that the first 50 m of E1-I withdrew about 10 times more heat out of the testbed than did the circulation of chilled water through the main fractures.

2.5 Repeatability

There was a lack of repeatability in early flow tests. A series of tests involving multiple injections, each lasting between four hours to two days (Figure 2.6), was conducted in the Spring of 2019 under very similar conditions (e.g., nominal rate of 0.4 L/min) to probe the testbed and evaluate reproducibility of its response. Although the testbed’s responses still varied among these tests, the replicate tests allowed differentiation of “systematic” responses from “random” responses. Four tests from this duration, initiated on February 21, February 26, March 19, and March 27 had long-enough previous shut-in periods for dissipation of overpressure in the system, were selected to construct Figure 2.7. As shown in Figure 2.7, three of these tests had very similar injection pressures while the pressure on February 26 was significantly higher. Another intriguing observation was that although the out-flow rates from the E1-P varied significantly; the arrival times were always two hours. These observations provide a sense of “variability” of the testbed’s response, critically important for holistic interpretation of other results from the testbed.

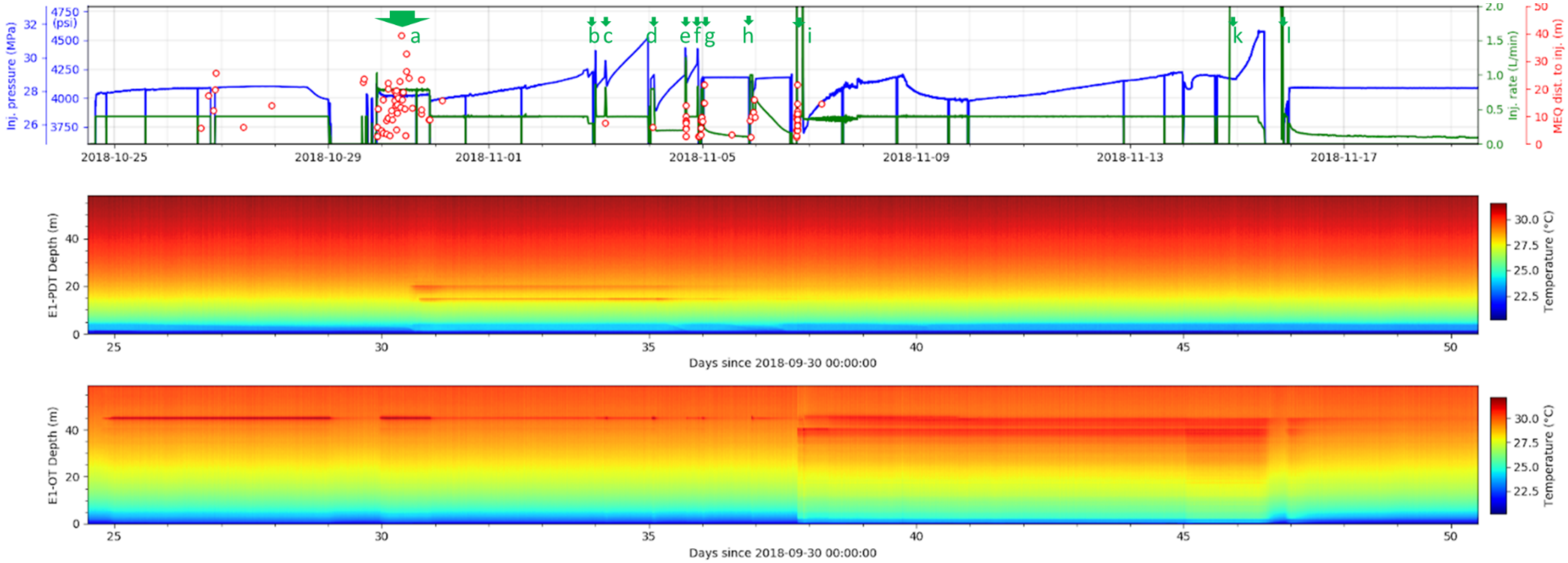

Figure 2.3: Synchronized flow data (blue line is pressure curve, green line is flow rate curve, and green arrowhead with markers "a" through "l" are periods of higher flow (=>0.8 L/min injection rates in the upper panel), MEQs (red circles in the upper panel), and DTS data from two wells (middle and lower panels). Each vertical line of DTS data show temperatures from the drift wall (lowest part of the panel – blue) to the deepest (top, red) at one time. Repeated measurements allow for the apparent continuous plot over time.

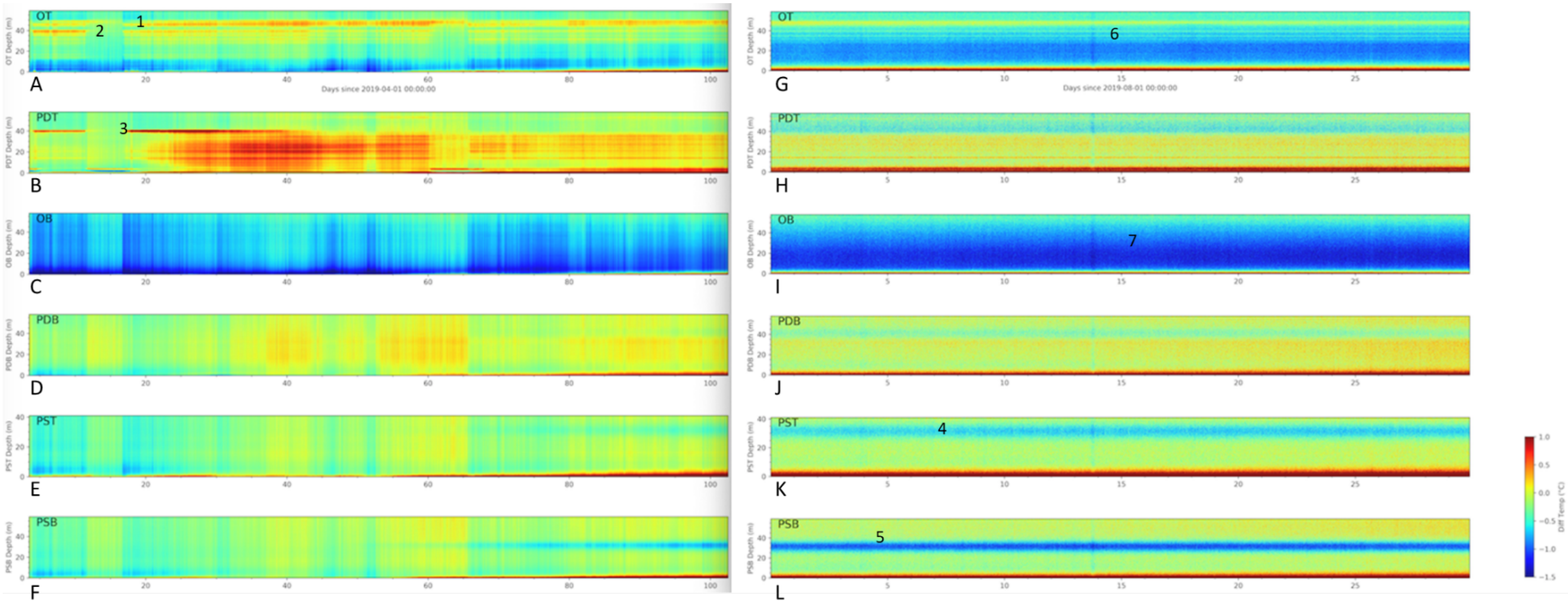

Figure 2.4: DTS measurements in terms of temperature change in six wells. The left panels (A-F) show results in April to June, and the right panels (G-L) show results in August 2019. Markers labeled as "1" through "3" point to warmer temperature anomalies whereas as "4" through "7" are cooler temperature anomalies.

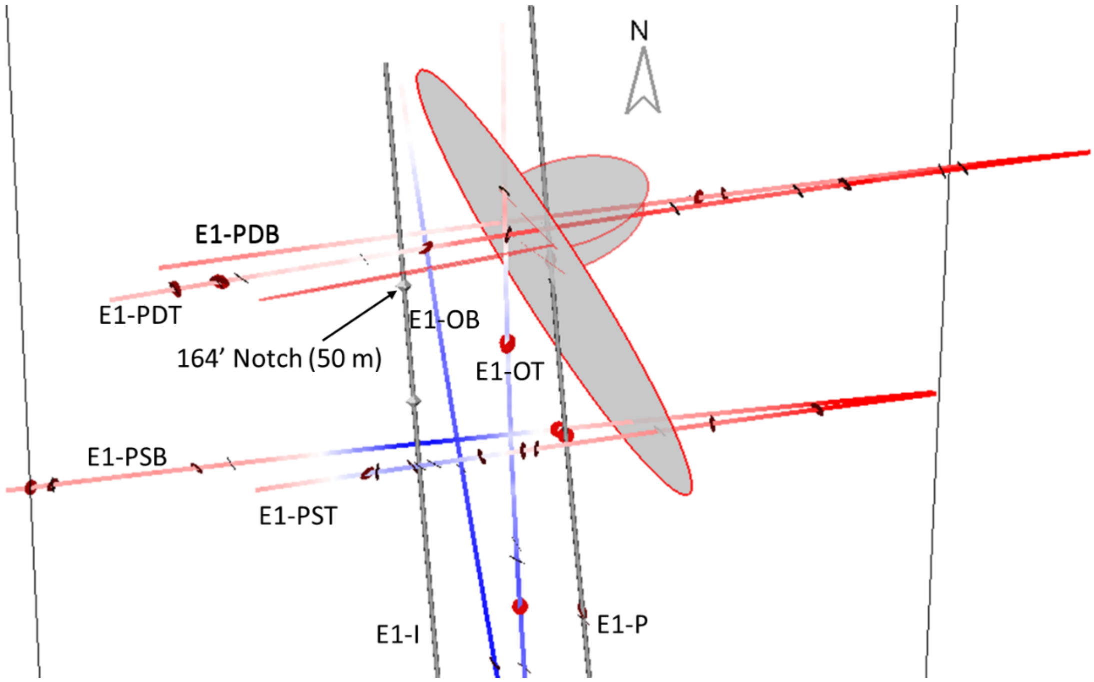

Figure 2.5: Spatially synchronized temperature data plotted on the trajectories of the eight wells, temperature change (blue meaning cooler and red meaning hotter than the background) along the six observation wells as of September 2019, logged open fractures along wellbores shown as small disks, and prominent hydraulic fractures stimulated in earlier experiments (larger disks). The chilled-water circulation in E1-I was limited to 164' Notch, and the deeper part of the hole was isolated from chilling.

2.6 Data Accessibility

A successful Collab experience is the systematic approach to make the data available as early as possible and available to as many people as possible. Different participants of the experiments, including modelers, experimentalists, geophysicists, hydrologists, senior scientists, graduate students, etc., contributed in different perspectives to the interpretation. Many important discoveries in Collab were made by the people who got opportunities to access the shared data.

To make data easily sharable and accessible, we encouraged all participants to use free and open-source data formats and upload the source and results to data storage and distribution system - the Data Foundry in OpenEI. The "Fat Crayon" toolkit developed for the design of the testbeds was written in Python and the outputs are presented in the open-source Visualization Toolkit (VTK) format. We also converted DTS data from Matlab and Python Pickle formats to a more accessible CSV format. Additionally, we devoted a significant effort to rapidly visualizing the complex dataset in an intuitively accessible way. Such a visualization is illustrated in Figure 2.8 where multi-stream datasets are used to create a series of diagrams for comprehensive understanding of the tests conducted over a long period.

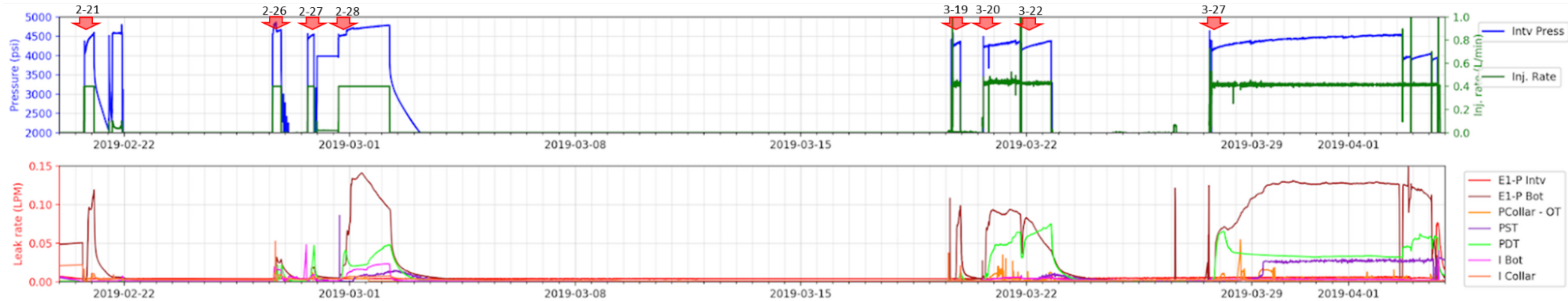

Figure 2.6: Injection and fluid recovery in a series tests conducted at 164' Notch in the Spring of 2019. The beginning of each separate tests is indicated by arrowheads and dates. The upper panel shows the injection pressure (blue) and injection rate (green). The lower panel shows the fluid recovery rates from several locations.

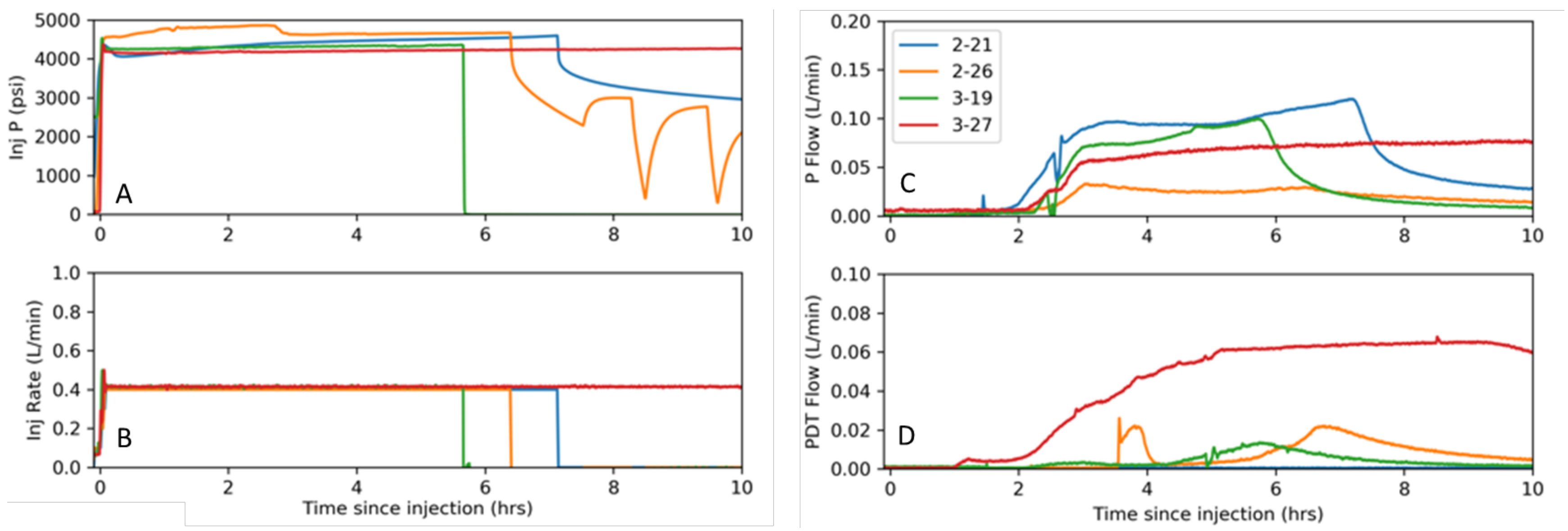

Figure 2.7: Results from four injection tests. Tests that followed other tests too closely thus not allowing overpressure dissipation were excluded. The horizontal axis is adjusted to make each test started at the origin. A) Evolution of injection pressures, B) constant injection flow rate, nominally set at 0.4 L/min, C) out-flow rate for E1-P, and D) out-flow rate for E1-PDT during these tests.

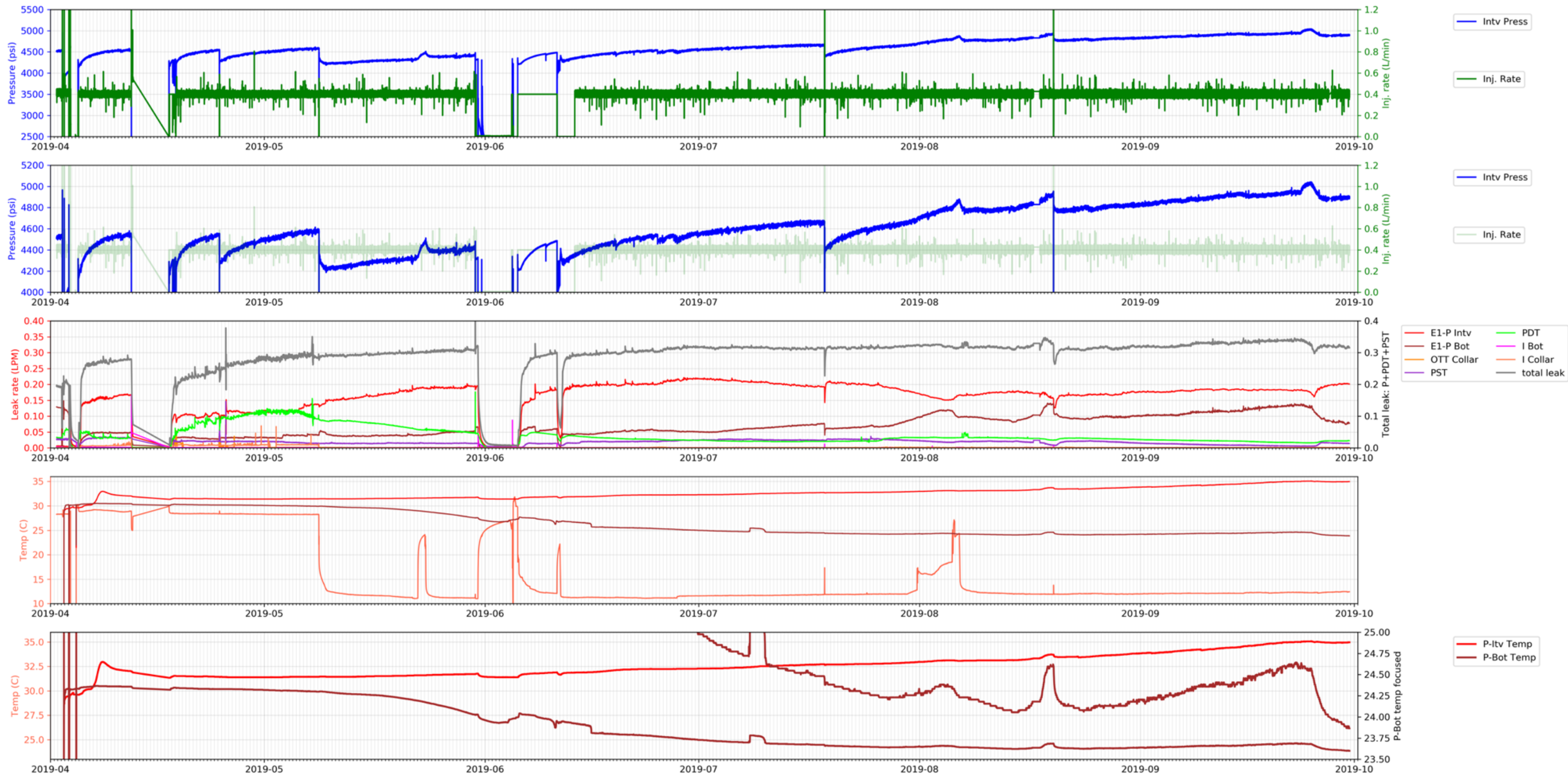

Figure 2.8: Multi-channel datasets are used to create a series of visualizations that are easy to understand and helpful to many data users. Included channels in this series of visualization are injection (E1-I interval) pressure and injection flow rate (top two panels), total and separate outflow rates from several producers (third panel from top), and E1-P interval (between packers) and E1-P bottom (below lower packer) temperatures (lower two panels) are shown for a period from April to October in 2019.

3. Seismic Data Processing

Abstract

An intensively equipped seismic monitoring system in Testbed 1 was deployed with a goal to image fracturing in the experimental rock volume through detection and location of microseismic events, as well as simultaneously acquire active seismic time-lapse imaging. The large number of sensors and their deployment in a 3D distribution around the stimulation zone via the 6 monitoring wells enabled rapid high-quality hypocenter determination with likely spatial resolution at the sub-meter level. Despite the challenges associated with sensor resonance, the accelerometer pods' high sensitivity allowed for production of an extensive event catalog that was refined by machine learning algorithms, thereby helping precise identification of hydraulic fracture planes, even those within proximity to each other. The value of these data was increased by an edge processing framework developed for Collab which allowed for near real-time event detection and location, a process which provided feedback into field operations. Edge analysis was required due to the very large data stream generated by 100 kHz continuous recording, required due to high event frequency. As a result, off-site data transfer was challenging but manageable.

3.1 Seismic Monitoring System

In the testbed, two of the six monitoring boreholes (Figure 1.2) were instrumented with strings of 12 hydrophones (HTI-96-Min) spaced 1.75 m apart and eighteen 3-component piezoelectric accelerometers (PCB 356B18) were deployed, with three accelerometers in each of the six monitoring boreholes (Schoenball et al., 2019b; Schoenball et al., 2020). Four 3-component geophones (Geospace GS-14L3, 28 Hz resonance frequency) were also deployed in shallow sub-vertical boreholes (Figure 3.1A). In addition, 20 automated seismic sources for CASSM were installed in the testbed. All sensors and active sources were attached to a 1-inch polyvinyl chloride (PVC) pipe and conveyed down the monitoring wells (Figure 3.1B).

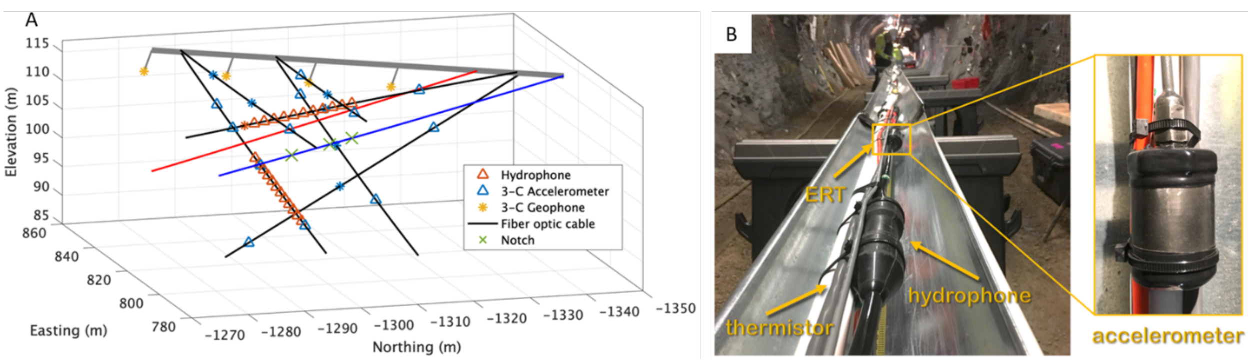

Figure 3.1: A) Seismic monitoring setup in Testbed 1 is comprised of hydrophones, accelerometers, and geophones. Stars (blue and orange) represent sensors connected only to the 4 kHz system that failed to produce useable signals. B) An assembly of monitoring strings with sensors fastened to PVC conveyance pipes prior to deployment in a monitoring borehole.

The seismic signals were recorded on a total of three digitizers and acquisition systems. The first system is a set of four Geometric Geode seismic recorders for a total of 96 channels and operating at 48 kHz sampling rate. The system operates in triggered mode to record the CASSM surveys. A second system, OYO GeoRes, is a conventional 96 channel exploration seismograph operating in continuous mode and at 4 kHz sampling rate. The third system, Data Translation

VibBox, is a high-performance 64 channel digitizer operating at 100 kHz with a 24 bit dynamic range. Due to the limited number of recording channels, only 12 of the accelerometers and all of the hydrophones could be connected to the 64-channel 100 kHz recording system. The remaining 4 channels were needed to record control signals of the active sources and the time signal. Further, one hydrophone failed, leaving us with 23 operational hydrophones. The 100 kHz system produced a data rate of about 25 MB/s which is stored on 8 TB external hard drives that were replaced every four days.

3.2 Passive Seismic Observations

During the stimulation test, up to about 10 seismic events per second were detected by accelerometer OT16. However, all other sensors produced inferior quality data. Hence, only a small fraction of events could be located. The detected seismic events have their peak energy around 10 kHz. The four geophones in shallow (5 m deep) holes did not produce useable signals, likely because of severe damping in the excavation damaged rock near the drift. Only data from the 64-channel VibBox system were used for seismic analyses.

For hydrophones, we observe a slight systematic dependence of the number of picks along each sensor string. Sensor-to-sensor variations of coupling appears to be more important for the usefulness of the recorded signals of the accelerometers. This is especially apparent for accelerometer OT16. In addition, the number of picks obtained from each station does not seem to vary systematically with the distance from the seismic events. For example, sensors OT18 and OB15 have vastly different performance, although they are close to each other and at similar distances to the seismicity.

3.3 Challenges in Signal Processing

One major challenge in seismic data processing is significant contamination with a variety of coherent noises, ranging from co-located sensor cross-talk to routine drilling and excavation activities in the vicinity of testbed. Particularly, cross-talk noise from high voltage ERT sensors produced thousands of false triggers per day. Jack-leg drilling activity with about 20 impacts (events) per second was found to be temporarily overloading the processing system with up to 100,000 events per day.

Signal discrimination between seismic events and noises used an approach that implemented and trained a discriminator based on principal component analysis (PCA) and a support vector machine (SVM) (Figure 3.2). This method utilized a training data set composed of 512 CASSM shots, 1140 drilling impacts, 3214 seismic events, and 5119 ERT cross-talk events. Since the noise signature is different on accelerometers and hydrophones but similar across sensor types we selected three traces of well-performing sensors (hydrophone PDB03 and the X and Z components of accelerometer OT16) and discarded the other traces. This reduced channel set is sufficient to discriminate the signals and it reduces the processing load needed for classification which is particularly important in the real-time application.

To extract each signal type's most salient features, we used PCA on a block size of 2 and a window size of 1700 samples, each event being represented with 849 components per channel. To classify the signals, we used a SVM where the primary mechanism involves identifying a hyper-plane separator which maximizes the distance between support vectors, or data points, closest to the separator. This binary classifier can be extended to multi-class cases by building "one-vs-all" classifiers. A grid search was performed by probing the performance of the SVM model across multiple parameter sets to find the best model. The final classifier is capable of correctly identifying more than 95 % of ERT and drilling noise. Once trained, the classifier can make its decision in about 0.1 s and is invoked before any picking routine is attempted. This reduces the processing load dramatically and guarantees a short latency between the seismic recording and event localization for real events of interest. The performance of the SVM classifier is promising for future applications.

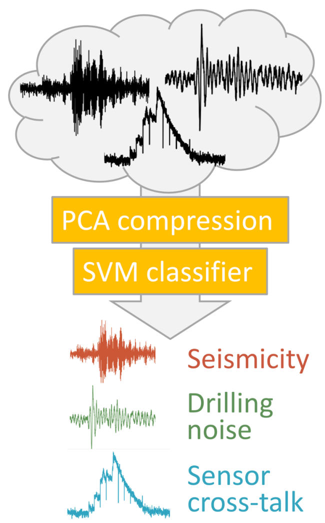

Figure 3.2: Workflow used for signal discrimination between seismic events and noise signals.

3.4 Lessons Learned and Way Forward

Collab Experiment 1 had an advantage that may also occur at FORGE at some point – the ability to ground-truth microseismic event locations. Our stimulated fractures intersected monitoring wells, and we were able to detect these intersections with non-seismic techniques (e.g. DTS) with fixed locations. This provided additional confidence in the microseismic locations, as well as an explanation of processes affecting the non-seismic data.

Different challenges in monitoring microseismicity will be encountered at FORGE. Well- and surface-based seismic monitoring at FORGE will not encompass the test region like what was done at Collab, and different noise sources will impact measurements. Continuous measurements may be able to utilize the noise sources however to detect changes in the reservoir. Machine learning algorithms may be useful at FORGE to identify important features in the data.

3.4.1 Data capture, storage retrieval, and sharing

One goal of the passive seismic monitoring was to continuously monitor long-term flow tests. To allow advanced processing such as ambient noise imaging and others to be applied in the future, we strived to collect the entire continuous data set with a full sampling rate of 100 kHz. However, this created challenges in data handling. To address this issue, we implemented an edge processing workflow which is capable of near real-time processing. It consists of a lightweight Python stack based on the ObsPy package (Krischer et al., 2015) that detects using a standard STA/LTA approach. Using a coincidence trigger that requires at least 20 components to trigger, we evaluate events that are strong enough such that an automatic picking algorithm based on the AIC picker would be able to determine P wave arrival times. If enough picks are obtained for an event, HYPOINVERSE (Klein, 2014) was used to determine its location. Then an independent 3-D viewer was used to read and plot updated location catalog (Figure 2.2). Although a conventional 8 core workstation located in the 4850 level drift was used to execute these algorithms within a couple of minutes (to up to 20 min delay when large numbers of seismic events were created during stimulations); the workflow can be optimized with parallelism to decrease processing delay and allow for a faster response.

After detection, the data are moved to a bank of 10 external hard drives. These hard drives were physically retrieved from the site with replacement of new drives to ensure continuous recordings. Overall, we achieved about 75% availability between May 21, 2018 and August, 2019. Critical phases of the experiment were covered with about 95% availability. To enable collaboration within the EGS Collab team and the larger community about 700 TB of the data has been uploaded to LBNL's 2 PB RAID server with sustained data transfer rates of 100 MB/s.

3.4.2 Selection of seismic sensors

An important lesson learned was on the frequency content of the passive seismic signals and the sensor response. For the monitoring of meso-scale testbed, only a limited range of sensors exist at appropriate frequencies. Seismic sensors sensitive in the 10 kHz range and above include piezoelectric accelerometers and piezoelectric acoustic emission sensors. Accelerometers work similarly to seismometers by having a mass moving against a piezoelectric crystal. The sensor response is determined by the mass of the sensor. There is a trade-off between a linear response to higher frequencies and the sensitivity of the sensor. A higher mass provides a higher sensitivity but leads to lower resonance frequencies, above which no usable signal can be retrieved. The selected accelerometers have a high sensitivity of 1000 mV/g but are specified to be linear only to 5 kHz and with resonance frequencies > 20 kHz. Our own measurements (Figure 3.3) indicate that the resonance frequency is much lower - at about 12 kHz for the Y and Z components and about 8 kHz for the X component. This is precisely where we observe most of the energy of the seismic events. As noted above, most seismic energy was detected in the 10 kHz range and energy at higher frequencies results from the resonances of the accelerometers.

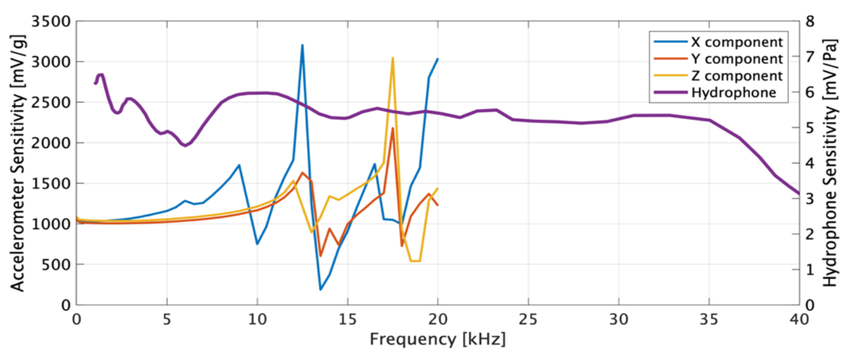

Figure 3.3: Frequency response curves of accelerometers and hydrophones deployed in Testbed 1.

For FORGE, well-behaved sensors, i.e. sensors that have a linear response in the target frequency range might help obtain better seismic signals. Accelerometers that are less sensitive but have a linear response function up to higher frequencies could serve for the FORGE. To retain or increase the overall sensitivity and record smaller events, these accelerometers would need to be combined with acoustic emission sensors. These sensors derive their signal as the incoming seismic waves deform the piezoelectric crystals which in turn generate a current. Such strategies have been successfully applied to other meso-scale experiments (Kwiatek et al., 2011, 2018; Villiger et al., 2020). Using this combination of sensors, meaningful magnitudes and even focal mechanisms would be possible to compute events down to the M^{-4} range.

3.4.3 Active source seismic and ERT interference

In Testbed 1, the CASSM system was continuously operated for most of the experiment and including parts of the long-term flow tests. Each CASSM shot occupies about 0.01 s and travel times to the sensors are less than 0.05 s. With about one CASSM shot per second, we incur only about 5% of downtime, during which the ability to record passive seismic signals would be impacted.

The cross-talk between the ERT system and the seismic acquisition provided for many challenges that are still not fully overcome. To be able to run both systems simultaneously, it is recommended that current pulses for both systems (ERT sensors and accelerometers) be measured on the same digitizer. Similar to the trigger for the active seismic sources, this signature should allow for an effective method to discard periods where the ERT system was active. Since each pulse only lasts for about 0.01 s, this would incur only minimal downtime and would enable monitoring the passive wavefield with about 94% coverage which includes downtimes during CASSM activity.

3.4.4 Machine learning

We are experiencing a revolution facilitated by successful implementations of Machine Learning (ML) applied to detection, phase picking and association to automatically detect and locate more (and smaller) earthquakes faster than before. At Collab, we have shown that ML can be used to bridge the gap between scales (Chai et al., 2020) by successfully applying ML models trained on regional scale earthquakes to the meso-scale, three orders of magnitude smaller. The accuracy of traditional automatic picking algorithms for low signal-to-noise data is often poor. This calls for manual review and refinement of phase picks. However, there is a fast-paced development of a new generation of picking algorithms based on deep learning methods. These have been applied with success by Chai et al. (2020) to the Experiment 1 data. After retraining the PhaseNet convolutional neural network (Zhu and Beroza, 2018) with the manually picked phase arrivals, the algorithm reaches human precision and surpasses the number of picks obtained by manual processing. Implementation of similar methods in real-time processing would be one of the next steps towards better and faster seismic monitoring. With the capability to detect smaller events, it becomes more likely that wave trains of events overlap across the sensor network. The association problem, that ties corresponding phase picks to events, has gained more attention recently and that can be useful for FORGE to discriminate between seismic events and noise sources, particularly if they occupy the same frequency band that is of interest for passive seismic monitoring.

4. Connecting Geophysics, Fractures, and Flow Systems

Abstract

A multi-pronged interrogation approach was implemented to characterize and monitor reservoir evolution during Experiment 1. The MEQ monitoring system (Section 3) was the primary tool used for imaging the propagation and extent of hydraulic fractures. Several additional measurements such as flowrate, pressure, and temperature, strain, tracers, and time-lapse ERT were conducted during the Experiment 1. This comprehensive monitoring system enabled us to compare the detailed testbed behavior described by data as a whole to corresponding inferences about testbed behavior derived from a single type of data (Section 2). Such comparison is useful for placing appropriate expectations, strengths, and caveats on inferences derived from a single data type and describe the integrated, consistent, and dynamic behavior of the testbed as revealed by different monitoring and characterization data sets. In this section, we briefly describe additional geophysical modes (besides MEQ) of monitoring flow during stimulations and flow tests to characterize fractures and flows in the testbed.

4.1 Distributed Fiber Optic Sensing

The deployment and utilization of multi-modal distributed fiber optic sensing better defined fracture interaction with the monitoring wells. During the experiment, temperature (DTS), strain (DSS), and dynamic strain rate (DAS) were monitored along all 6 monitoring wells, with DTS running for the entirety of the testbed lifetime. This measurement suite, particularly the DTS, provided key constraints for fracture/well intersections within the testbed. The DAS & DSS provided additional information constraining near-wellbore deformation; the DAS dataset appears promising as a tool to examine fracture interaction and analysis of this data set continues.

The DTS dataset was acquired at a 25 cm spatial resolution and a 10-minute time resolution, thus providing a near-real-time map of fluid movement past the 6 monitoring wells, mainly through Joule-Thompson effects discussed in Section 5.3.1. The 25 cm spatial resolution allowed integration of DTS with fracture features mapped through both borehole image logs as well as microseismic measurements. Significantly, the temperature signatures measured with DTS were directly associated with fluid flow rather than seismicity, thus providing a detailed record of fluid movement at well bores sampling the stimulated volume.

Away from the locations of individual fluid "hits" on the DTS, there was also a general background trend in the evolution of temperature in the testbed. Early in the project, it was presumed that this background trend would be heavily influenced by the discrete fractures and, consequently, would be highly heterogeneous. However, when the DTS data were projected into 3D space, it was found to be consistent with more conductive cooling resulted from circulation of cold water in the E1-I (Section 2.4). Slower and more spatially distributed evolution of the rock mass temperature informs our understanding of how fractures and other heterogeneities are reducing the uniformity of heat extraction.

4.2 CASSM

The CASSM measurements, utilizing the seismic sensor network and 20 active sources which were intermittently excited, was successful and detected both velocity and reflectivity changes associated with the stimulation stages. Figure 4.1 shows the result of a CASSM inversion after the May 2018 stimulation sequence, demonstrating a reduction in compressional wave velocity (Vp) associated with a newly created fracture, as well as the passive microseismic data. Significantly, the same experiment allowed monitoring of the recovery of the Vp perturbation during shut-in as the fracture aperture decreased. This is an example of effective monitoring of aseismic mechanical property changes in the fracture network at a distance from the borehole, a step closer to understanding the flowing fracture distribution.

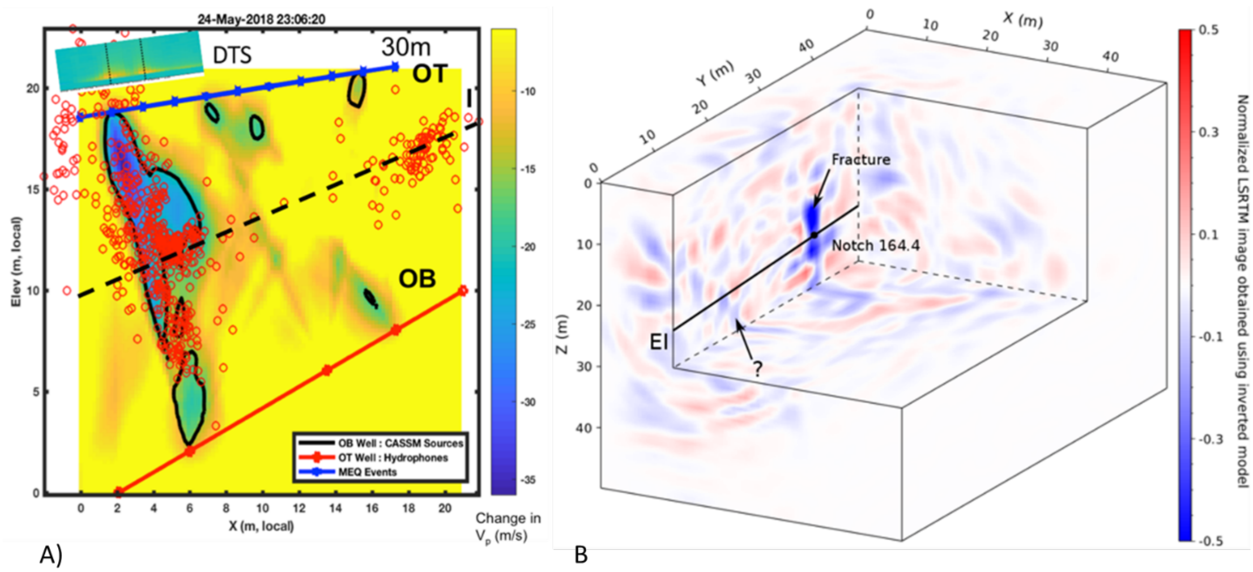

Figure 4.1: A) An image showing the changes in Vp induced during the first (May) stimulation sequence as imaged by CASSM and validated by microseismic locations (red circles) and DTS (along OT upper left corner). The imaging plane is between monitoring wells OT & OB, obliquely crossing the OT-P connector fracture plane. As can be seen, all three datasets provide a consistent picture of the fracture system. B) Least-squares reverse-time migration of CASSM data acquired using hydrophones and accelerometers at 22:29:19 and 22:47:47 on 5/24/2018 and anisotropic elastic-waveform inversion results, revealing the fracture created by hydraulic fracturing at the 164' Notch, and some other possible existing fractures.

4.3 Strain Measurements at the Borehole

Direct measurement of displacement on fractures during stimulation and flow can inform interpretation of normal versus shear stimulation. During stimulation and flow, strain measurements were taken across individual fractures using the SIMFIP tool. While data could be retrieved from the SIMFIP tool in real time, interpretation was performed offline, making it a qualitative measurement during stimulation. The measurements provided some constraint but were sometimes difficult to interpret because the testing zone contained multiple features. In some cases, it was possible to perform analysis of the SIMFIP results that informed the stimulation processes (Guglielmi et al., 2020). It is expected that over time, SIMFIP measurements will be more rapidly interpreted allowing for routine use in observing stimulations.

More distributed displacement measurements across multiple fractures could be informative as well, especially if the data can be interpreted quantitatively in real-time. For example, tools are emerging that provide distributed displacement measurements via a network of fibers pressed against the borehole wall (https://lunainc.com/blog/luna-and-shell-gamechanger-innovate-new-underground-sensor).

4.4 Electrical Resistance Tomography

The ERT characterization and monitoring system in the testbed included an array of electrodes grouted in place within the six monitoring wells, with 16 electrodes per well. These electrodes enabled characterization of the 3D low-frequency electrical properties of the host rock, and changes in those properties during stimulation and tracer testing using both static and time-lapse ERT (Johnson et al., 2019).

Figure 4.2 shows baseline ERT images of the Testbed 1 collected prior to stimulation and flow testing. The ERT images suggest the testbed is oriented within a zone of folded layers of alternating high and low electrical conductivity, with the axis of the fold dipping downward toward the northwest. Borehole electrical conductivity logging results, also depicted in Figure 4.2A, display good agreement with the ERT image. In Figure 4.2B, natural fracture locations and orientations derived from core inspection superimposed on the baseline ERT image suggest the primary natural fractures strike parallel to the high/low conductivity layers. These natural fractures play a governing role on fluid flow within the system.

Figure 4.3 presents one image of a time-lapse 3D ERT series showing the change in bulk conductivity within the testbed during a post-stimulation flow test. Fluid was injected into previously stimulated interval of the injection well (164' Notch). During stimulation and subsequent flow testing, MEQs occurred predominantly along the anticipated hydraulic fracture plane. The warm colors in Figure 4.3 show an increase in bulk electrical conductivity, which is caused by either an increase in fracture fluid conductivity or an increase in fracture aperture, or both in comparison to baseline.

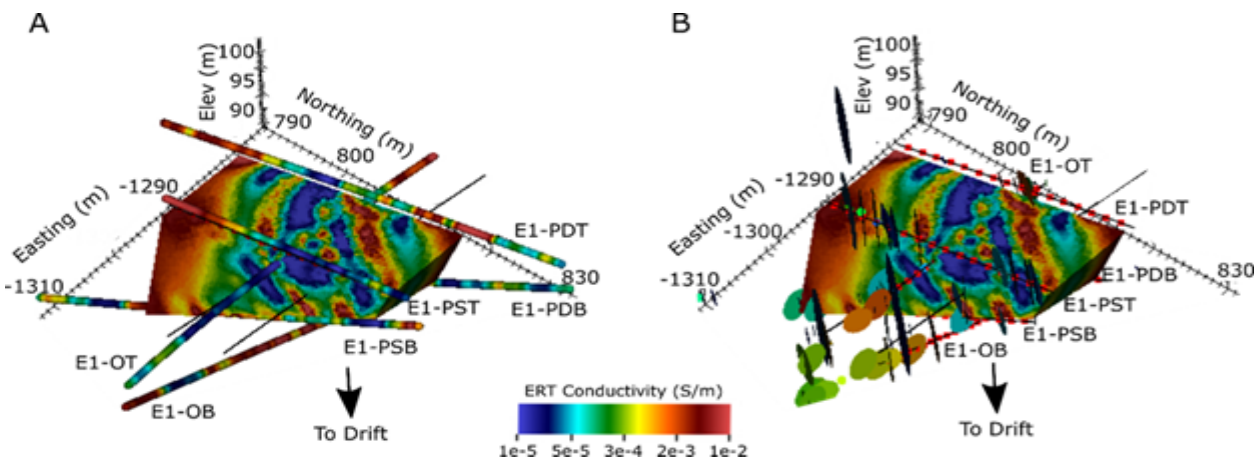

Figure 4.2. A) Baseline ERT image of Testbed 1. Borehole EC logging displayed in color scale along the monitoring wells display good agreement with the ERT image. B) Natural fractures (black discs) strike parallel to the high/low conductivity layers identified in the ERT image.

The ERT time series (Johnson et al., 2019) shows the increase in conductivity originating along the stimulated fracture plane in early time and then migrating to the southeast along the natural fracture planes as more fluid was injected into the 164' Notch. This suggests that the stimulated fracture connected with the natural fracture system, which then provided the dominant fluid flow paths. This conclusion is supported by other point sensing modes including DTS data which suggest a strong hydraulic connection between well E1-OT and E1-P along the natural fracture zone. In this case, the MEQ data were effective at validating the presumed location, orientation and growth of the stimulated fracture zone, but they were less effective at informing actual fluid flow paths, particularly when those flow paths existed primarily within natural fracture zones. These results suggest care should be taken when inferring fluid flow paths in the reservoir based on MEQ data alone.

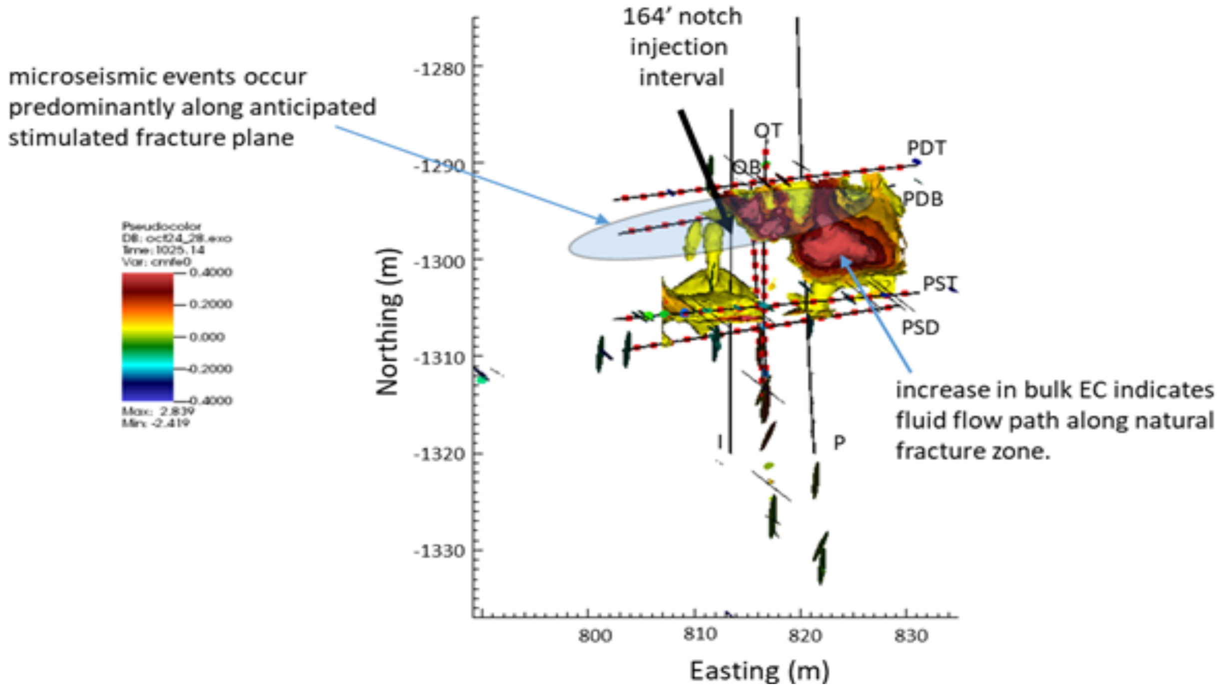

Figure 4.3: Time-lapse ERT image collected during a flow test suggests the stimulated fracture intersects a natural fracture zone, which largely governs fluid flow.

4.5 Challenges of Characterizing Fractured Flow Systems and Lessons Learned

Direct observation of complete cores, interpretation of image logs, fracture/shear zone mapping in the vicinity of the testbed, and a range of geophysical and hydraulic measurements including tracer tests were employed to characterize the natural as well as created hydraulic fractures and flows in the testbed. These data sets were then integrated into a discrete fracture network model, which served as the basis for conceptualizing fracture flow pathways. Despite being able to characterize and monitor major natural and created fractures at individual levels, there still exist challenges in unraveling the thermal exchange/heat extraction characterization of the reservoir fracture system in the testbed.

Reconstruction and orienting core provide key information on the subsurface environment. This task needs to be performed in a timely manner as it provides ground-truth information. Correlating it to wireline measurements allows extension of the ground-truth information and more reliable interpretation of the wireline data. Geophysical sensors must be appropriate for the precise situations they are applied in. Time-lapse measurements using multiple techniques including simple hydrological to geophysical methods improve understanding of the initial system *and* changes. At FORGE, repeat and similar measurements should be jointly interpreted when new data become available to identify changes in the subsurface system. Joint interpretation of multiple data streams is key to providing additional understanding. Adequate emphasis must be placed on the ability to process the collected data.

Not all the techniques used in Collab are directly applicable at FORGE because of the temperature at FORGE and cost of application. Combined fiber optic sensing has been extremely valuable at Collab and is likely compatible for the operating conditions at FORGE, and for the low-cost relative to the quality and quantity of data collected. Rapid sharing of data at FORGE might be difficult because numerous parties will be collecting data. A unified data collection and sharing platform where data must be rapidly posted and shared would help in understanding the FORGE reservoir.

4.5.1 Lessons Learned: understand the pre-stimulation rock volume, core and borehole characterization and correlation with wireline measurements

The near 100 percent core recovery in both Testbeds 1 and 2 provided opportunities to characterize the rock and the natural fractures present in the testbed. Optical and acoustic televiewers proved to be an excellent means of correlating core and wireline observations allowing the core and the fractures present in the core to be oriented. Although the core continuity was maintained from one core run to the next by matching the core ends, orienting the core was slow. This reduced the utility of the observations, and progress would have benefited by having a better system for making those observations and orienting the core in a timely manner. The cores also provided material to determine the mechanical properties of the rock through a range of very different compositions.

Natural fractures in Testbed 1 were created during a long geologic history beginning in the Precambrian and including a significant fracturing episode during Tertiary time. The fractures ranged from 1-3 m thick shear zones, probably associated with Precambrian shear zones reactivated during Tertiary time, to open fractures, to thin healed fractures with little permeability, which may not be mechanically weaker (Frash et al., 2019; Ye et al., 2019). Examination of the fractures in the core provided insights in the mechanism for fracture development (Roggenthen et al., 2018), which in the case of Testbed 1 involved dissolution along shear zones with subsequent precipitation of secondary minerals in portions of the produced porosity. In contrast, the more open fractures do not appear to be associated with the shear zones and have little filling material inferring that their extent may be more limited. During the tests, a small number of fractures controlled the flow in the testbed, and the major flow paths changed over time. Thus, examination of the fractures and their orientations provides clues as to which fracture sets are more likely to be transmissive over longer distances.

4.5.2 Moving Beyond an Initial Model to Understand Flowing Fractures: Geophysical Constraints on the Dynamic Fracture Systems

Understanding Testbed 1 benefited from an extensive three-dimension monitoring network as discussed above. These systems were utilized to acquire an integrated active/passive seismic dataset, a range of fiber sensing measurements, and time-lapse ERT data. The target of these measurements was to monitor the evolution of the dynamic fracture network at the testbed.

Lesson learned: Lack of data from near-drift sensors

In addition to the borehole 3-component (3C) accelerometers and hydrophones used for MEQ detection, a sequence of shallow wells was emplaced in the drift and equipped with 3C geophones. These geophone sensors did not record useful data, i.e., they did not detect any MEQ or CASSM source pulses and measured only noise in the drift from human activity. Several important lessons were learned from this experience, mainly (a) deployment of sensors in the relatively low Q near-drift environment greatly reduced sensitivity, and (b) geophones are not optimized for the higher frequency signal content of low magnitude events.

Lesson learned: ability to process data

Several data streams, CASSM and DAS data in particular, require extensive method development and human resources to effectively process the data. The results from these data sources, which would have been useful for managing stimulation, could not be effectively fed forward into operations. For future pilots, we would recommend early investment in (a) real-time processing infrastructure to make these and other rich datasets more quickly available and (b) more effective mapping between data streams and personnel to reduce "orphan" datasets.

Lesson learned: new techniques and joint inversion

MEQ and flow processes near monitoring wells indicated by DTS helped delineate the creation of the fracture network. More novel techniques were piloted in the hope of geophysically imaging flowing fractures in the testbed. CASSM data was acquired to image changes in Vp and shear wave velocity (Vs) associated with changes in fracture aperture, which can in turn be related to local fracture permeability. Continuous ERT data were acquired in the hopes of imaging changes in fluid conductivity associated injection of low-EC or mine water. Consideration of new monitoring technologies such as these under EGS conditions should be considered in the ongoing plans for FORGE.

As discussed in Section 4.4, the dynamic ERT utilized a multi-well array of grouted electrodes to image changes in electrical conductivity as a function of time. Due to the difference in fluid conductivity between injected and native fluids, flow within fractures is visible as changes in conductivity. A fracture between wells E1-P and E1-OT was resolved by MEQ, CASSM, and DTS. This can be seen during aseismic flow operations using ERT. One goal which has not yet been achieved is joint inversion of these disparate datasets which should cross-constrain each other, rather than simply validate.

Lesson learned: instrument interference

Another challenge encountered was the issue of instrumentation cross-talk in the heavily utilized boreholes, particularly between ERT acquisition and microseismic measurements. ERT cycles were flagged as events in the automated microseismic analysis system and needed to be removed in a post-processing step. We recommend that future studies (a) acquire ERT waveforms on the seismic acquisition system to allow for trigger rejection and (b) explore techniques to reduce electrical interference between these systems. On a positive note, the fiber optic systems (e.g. DTS) are purely optical systems and are insensitive to electrical noise.

Suggestions for FORGE: fit-for-purpose geophysics for fracture monitoring

While we have documented a variety of monitoring successes (and failures) at Testbed 1, not all of these approaches will be directly transferable to FORGE. Some of the successes were related to our capacity to use a large number of highly instrumented dedicated monitoring wells (6) to fully surround the target zone with sensors. This approach also enabled deployment of relatively new techniques such as CASSM & dynamic ERT for one of the first times in a complicated geothermal testbed. For deeper EGS experiments, drilling costs are a significant constraint and not every instrumentation component can be utilized at higher temperature.

Of the methods piloted, the combined fiber optic sensing package is perhaps the most obvious extension to FORGE; modern fiber optic cables equipped with polyimide-coated fibers can perform well at high temperatures (up to 300 ºC). DTS data can aid in understanding spatiotemporal variations in fracture flow in the near-wellbore regime. DAS measurements, which were also conducted at Collab, would in fact be better suited for the length scales at FORGE. DAS has a relatively long spatial averaging scale (referred to as a gauge length, ~10 m at Collab) which is a poor match for smaller target zone and shorter Collab wells. However, this will not be an issue for FORGE which is targeting longer distances and lower frequency microseismic events. Fiber strain (DAS & DSS) can also be used to detect fracture deformation, an advantage at FORGE where secondary geodetic systems are complicated to deploy.

Effective multi-instrument packages in a smaller number of wells can provide datasets with maximum value optimized cost constraints. Information at depth proved particularly valuable; high quality microseismic measurements were crucial and provided one of the highest resolution pictures of the active components of the fracture network, at least during the phase when new fractures were being created. If a system fitting the appropriate characteristics is deployed at FORGE, a method similar to an edge processing framework would provide high-quality hypocenter (and perhaps magnitude) data during stimulation operations. We would also recommend deep sensor deployment; as mentioned previously, our drift recordings (shallow) using geophones were entirely unsuccessful (due to low Q & sensor properties) and the best results were obtained from sensors close to the stimulation zone tuned for the higher frequency content of the low magnitude seismic activity.

A challenge at Collab and fractured sites was our capacity to resolve flowing fractures vs. zones of failure with low permeability. We were aided by excellent constraints at wellbores (e.g., DTS) and the availability of localized fracture mechanical parameters (e.g., CASSM) and fluid movement information (e.g., ERT and tracers). Geophysical approaches which can access constraints on fluid flow at remote locations, particularly considering the challenges related to performing multi-level hydraulic tests in hot borehole environments could be considered at FORGE.

All of these techniques do have challenges for high temperature operations but these can be overcome in some situations. The limitation in CASSM is the development of a high temperature borehole seismic source. Recent advances in piezoceramic materials suggest that such a source is a reasonable goal, particularly for intermediate temperatures (180-220º C). For ERT, current cable technologies are likely sufficient but electrode reactivity may be a challenge. In either case, such technologies might be candidates for deployment in future FORGE test wells.

5. Challenges of Modeling Fractured Flow Systems

Abstract

In the Collab project, numerical simulations were successfully executed to: 1) support experimental designs, 2) estimate the magnitudes of the effects of the applied stimuli to obtain approvals to proceed, 3) forecast outcomes of operational changes, and 4) provide understanding of observed behaviors. Validation of numerical simulation tools is a stated objective of the Collab project, with the principal objective of learning whether the capabilities of modern state-of-the-art simulators are sufficient to accurately predict stimulation, fracture networks, and subsequently thermal energy recovery for the Collab experiments. No grand-scale validation test has been performed comparing simulations and measurements for an entire experiment yielding approved validated software packages. Validations have instead been performed stepwise generating a high degree of confidence in the ability of experienced modelers to use the simulation tools which require intermittent improvement to generate reasonable solutions and estimates. Thus, numerous simulations have provided many validations - to the extent that the simulators, used by experienced modelers seeking mechanistic explanations, provide useful information for planning, interpretation, and process quantification and understanding. The ability to perform near-real-time simulations to provide suggested explanations to observations attests to the confidence in the simulators, and the modeling and simulation *process*.

Numerical simulation is an essential component of the Collab project and has earned confidence because modelers began with detailed understanding of the experiments and expert use of codes that incorporate known processes to the extent reasonable to produce near-real-time reliable high-quality solutions to a team that understands the value *and* shortfalls of the modeling efforts. It is understood that unknowable heterogeneities in the rock fabric, natural fractures, spatial variations of in-situ stress, and other geologic features generally preclude numerical simulation from providing accurate matches to experimental outcomes. The true value of numerical simulation comes from the understanding it provides concerning complex system behavior, allowing scientists and engineers to make informed choices about experimental designs and interpreting experimental observations.

There are many remaining challenges in simulating fracture flow and heat extraction. Understanding the interplay between poroelastic, thermal, chemical, and biological processes is key to interpreting injection-pressure data. The rates at which chemistry may impact flow can be surprisingly fast, complicating the interpretation of injectivity data. Water chemistry and its interactions with the engineered systems and the formation need to be understood. In spite of the measurement techniques available, it is not possible to provide boundary condition measurements on the scale that a mechanistic model may require. Thus, a disjoint likely exists between actual and model boundaries. Reducing the severity of this disjoint is important for determining whether that difference or modeled processes are responsible for observations.

Another remaining challenge is modeling a dynamic system. Over time, the locations where water was collected changed. It is not clear whether processes already included in the simulators are responsible, or other processes. Without additional observations and data, one can only speculate on the causes. The models however can be used to offer insights into processes and their magnitudes, and provide a guide to the next measurements needed.

Application of these simulation tools to FORGE or other sites with elevated temperatures will require additional stepwise confidence building in the hands of an experienced modelers knowledgeable of the processes requiring consideration. If this is performed, the process is likely to be successful.

5.1 Pre-stimulation Numerical Modeling

Numerical simulations were executed prior to hydraulically stimulating the experimental volume to answer specific questions:

1. What are the anticipated number and magnitudes of seismic events during hydraulic stimulation (Zhou et al., 2017; Huang et al., 2018)?
2. What is the thermal profile in the Testbed 1 (White et al., 2019)?
3. What will be the fracture geometry from the well will a transverse hydraulic fracture form from the unaltered injection borehole drilled in the direction of minimum horizontal stress, or is notching required (White et al., 2018; Fu et al., 2018)?
4. How does notch geometry impact stimulation pressure and near wellbore impedance (White et al., 2018)?
5. How is the stress state altered in the experimental volume via mechanical and thermal alteration from the mine workings and drift cooling (Fu et al., 2018; White et al., 2019)?
6. What is the preferred orientation for the stimulation borehole to meet the project objectives (Knox et al., 2017; Morris et al., 2018)?
7. What flow rates and pressures should the circulation experiments be executed at to prevent fracture propagation (Fu et al., 2018; White et al., 2018; Huang et al., 2018)?
8. What circulation duration is required to achieve measurable temperature changes in the production borehole (Zhang et al., 2018; Kutun et al., 2018; Wu, Y.S., et al., 2020)?
9. Can the production well serve to prevent fracture propagation to the drift (White et al., 2018)?
10. What is the anticipated fracture shape and arrival time in terms of injected fluid volume of the hydraulically generated fracture under the mechanically and thermally altered stress state (Fu et al., 2018)?

The following sections describe the numerical simulations performed to resolve four of these questions. For other questions, additional details can be found in the references cited above. In addition, mechanistic modeling to interpret stimulation data and better understand fracturing behaviors has been performed using a series of 2D and 3D simulations. These simulations use coupled conjugate network flow and quasi-static discrete element model (DEM). The fracturing behaviors of naturally fractured crystalline rocks under hydraulic stimulations are investigated by systematically varying geometrical, hydraulic and mechanical attributes of natural fractures (Huang et al., 2019).

5.1.1 Seismic events and magnitudes during hydraulic stimulation

The question of what the anticipated number and magnitude of seismic events associated with the hydraulic stimulation was answered with numerical simulations executed with a fully coupled three-dimensional network flow and quasi-static discrete element model (DEM) (Zhou et al., 2017; Huang et al., 2018). The simulation is initialized by imposing the in-situ stresses as strain energy in the elastic beams connecting the DEM particles. As the beams break with fluid injection, this strain energy is released. Estimates of the magnitude of the seismic events that occurred during the stimulation were developed by considering each beam break as an event, or by summing the released energy over a time step. The outcome from these simulations forecast a maximum energy release during stimulation to occur during the initial fracture opening state of about 37.5 kJ, which is equivalent to a 0.1 magnitude on the Richter scale. The simulations additionally showed that after the initial opening, the fracture propagates smoothly (on average) under constant rate injection, with a few relatively large events.

5.1.2 Thermal environment surrounding the drift

Unaltered ambient temperature of the testbed at the 4850 level, determined from the Homestake mine surveys, is approximately 34˚C. Drifting activities started at the 4850 level in 1949 and a variety of active cooling systems were used to reduce working temperatures for the miners. The temperature profiles surrounding the 4850 level drift are a function of the early mining activities from 1949 through 2003, the mine closure from 2003 to 2009, and then the reopening of the 4850 level for scientific and engineering research from 2009 to present. Predictions of the temperature profile around the 4850 level drift were made via numerical simulation and verified against DUSEL, kISMET, and Collab boreholes temperature logs (Dobson and Salve, 2009; Oldenburg et al., 2017; Roggenthen and King, 2017) from the Experiment 1 Testbed (White et al., 2019, Figure 5.1). The computed thermal profiles surrounding the drift were subsequently used to compute the altered stress state surrounding the drift and its impact on the hydraulic fracture geometry, and for modeling thermal circulation experiments (e.g., Fu et al., 2018; Wu, Y.S., et al., 2020).

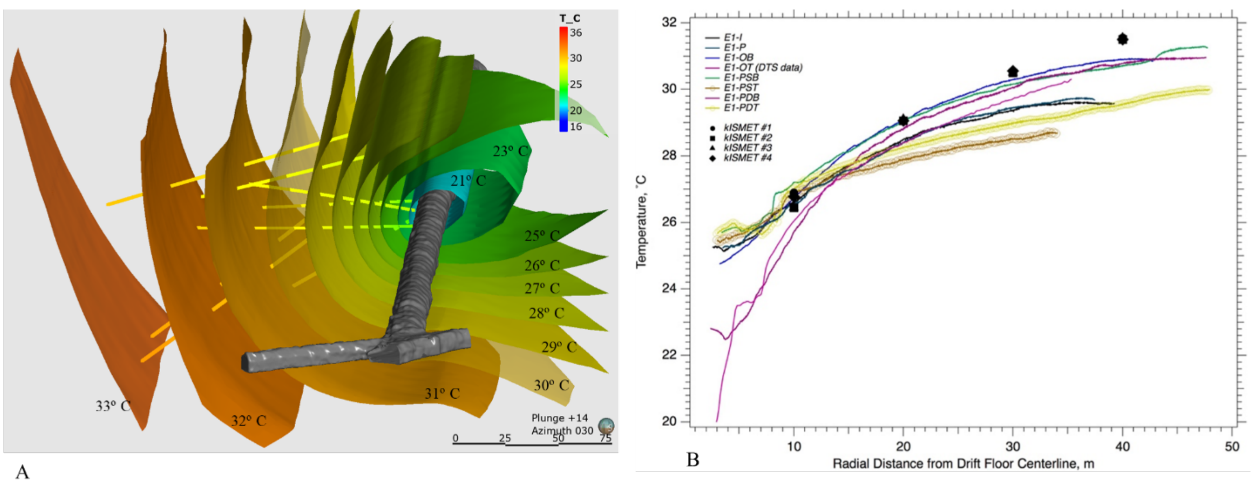

Figure 5.1: A) Comparison of temperature profiles within the testbed volume from numerical simulations and temperature logging of the boreholes. Image generated with Leapfrog Software. B) Comparison of temperature profiles as a function of radial distance from the drift centerline, including kISMET boreholes.

5.1.3 Impact of Borehole Notching on Fracture Initiation

Borehole notching design was investigated to generate the stress concentration that was thought to be necessary for initiating a hydraulic fracture perpendicular to the borehole direction because pressurization of a smooth borehole, cylindrical in shape, has very little effect on the axial stress along the borehole according to Kirsch's equations. Various notching mechanisms had been considered, including abrasive perforation, shape charges, and mechanical notching. Due to the desire to avoid explosives and logistic complexities, mechanical notching was considered as a favorable solution. The objective of this numerical study was to quantify the effects of notch geometries on stress concentration near the notch when both the borehole and the notch were subjected to fluid pressure. The study comprised a parallel stress analysis and fracture mechanics analysis, which involved introducing a 4-mm deep crack at the apex of the notch (Figure 5.2). A series of simulations was executed to generate the coefficients of a transfer function that allowed the calculation of tensile stress at either point A or B over a range of notch geometries and fluid pressures, which took advantage of the linearity of the system (White et al., 2018). The principal concern for the Collab team was whether an axial fracture would develop and propagate before a transverse fracture could be initiated at the notch. A fluid pressure of 35 MPa was selected for the study, which was lower than σ_h or σ_V, which guaranteed that no axial fracture could propagate. The study concluded that the 35 MPa fluid pressure could generate sufficient tensile stress, for all notch geometries considered, to generate a transverse fracture from the notch prior to generating an axial fracture. This conclusion applied even if there already existed an axial fracture or a fracture that intersected the borehole and was sub-parallel to the borehole. Ultimately, triangular cross-section notches were used to initiate the fractures.

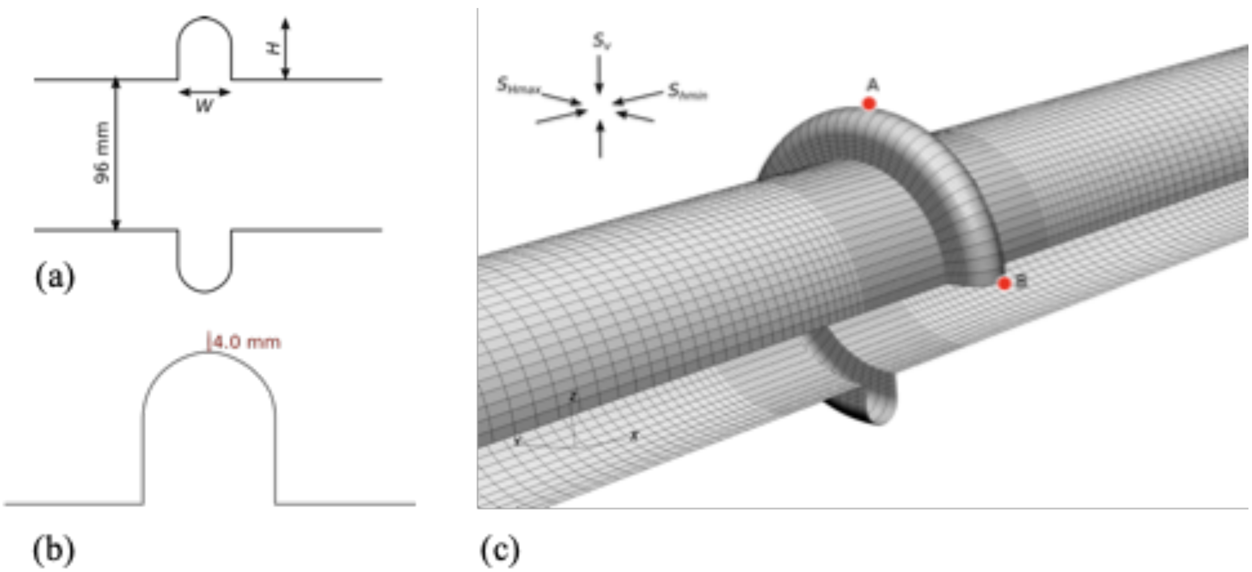

Figure 5.2: Notch geometry considered in this analysis. (a) A smooth notch surface for stress analysis with notch depth H and notch width W as variables. (b) Assuming a 4-mm deep crack at the crown of the smooth notch for fracture mechanics analysis. Illustration not to scale, (c) Mesh of the "skin" of the borehole and notch with H = 20 mm and W = 20 mm.

5.1.4 Fracture propagation around a production borehole

The GEOS code (Fu et al., 2013; Settgast et al., 2017) was used to investigate the ability of the production borehole to arrest fracture propagation toward the drift. The experimental protocol strategy was to maintain the production borehole at a constant pressure, slightly below σ_h, via a combination of a low-flow injection pump and a pressure relief valve, and then monitoring for fracture arrival at the production borehole via a change in drainage flow rate out the pressure relief valve. Numerical simulations were executed to address three questions: 1) what impact does production borehole drainage on continued fracture propagation, 2) what is the drainage rate from the production borehole at fracture arrival, and 3) what are the effects of back-pressure and injection rate? Conclusions from the simulations (White et al., 2018) indicated the production borehole could serve as a barrier to continued fracture propagation. In addition, numerical simulations showed:

- The flow rate into the drainage well is not very sensitive to the back-pressure applied in the well.
- The halting effects of the drainage well are more significant for lower injection rate.
- For very low injection rate (e.g., 0.02 L/s), the drainage rate can be 70% of the injection rate and fracture growth in other directions are also substantially impeded.
- If a five-spot configuration is adopted, the overall fracture growth can be halted in almost all directions.

Laboratory experiments also resulted in the conclusion that production boreholes can "cage" developing fractures (Frash et al., 2018a, b; Frash et al., 2020).

5.2 Numerical Simulations to Forecast Outcomes of Operational Processes

Numerical simulations were executed to forecast the development of the fracture network within the testbed, both considering and ignoring natural fractures. These simulations followed an iterative process (White et al., 2019), modifying conceptualization of the experimental testbed, but also capabilities of the numerical simulators in response to experimental observations.

5.2.1 Fracture propagation under a thermally altered stress gradient

Prior to selecting the site for the EGS Collab Experiment 1 numerical simulations were executed to forecast fracturing pressures, fracture propagation, fluid circulation rates, and thermal drawdown (White et al., 2018). In general, these scoping simulations considered vertical gradients in stress and mechanical stress alterations due to the mine workings but not the stress alteration due to thermal cooling of the experimental rock volume from the drift. The resulting fractures from these scoping calculations were generally penny shaped (Figure 5.3b). A numerical analysis by the LLNL team additionally considered the impact of stress heterogeneity, by assigning a randomly generated heterogeneity with standard deviation of 0.5, 0.25, and 0.125 MPa on σ_h. These simulations revealed the strong impact of stress heterogeneity on fracture shape, aperture, and circulation flow rates (Figure 5.3a).

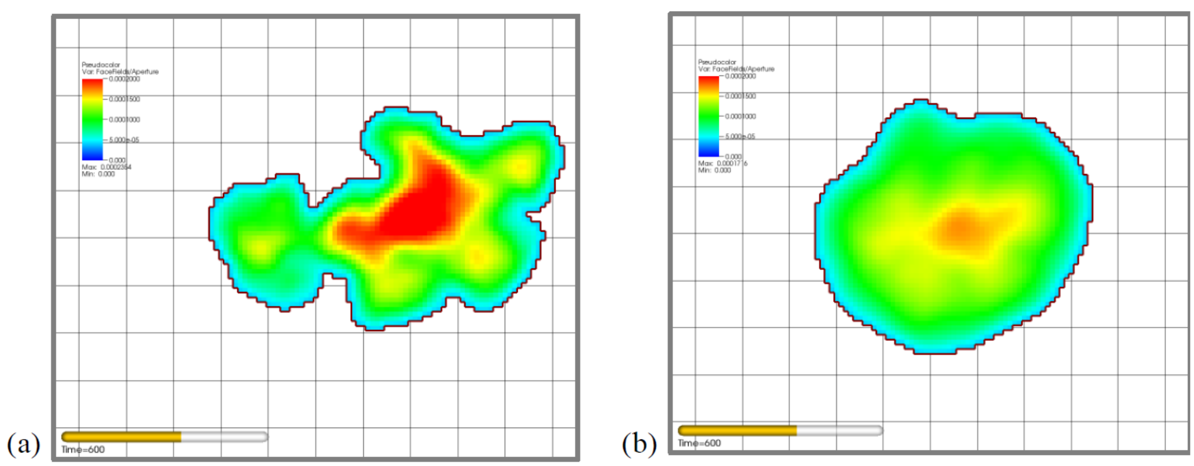

Figure 5.3: Numerical simulation of fracture propagation with different realizations of s_h with a mean of 20 MPa, and vertical gradient of 14 kPa/m (a) standard deviation = 0.5 MPa, (b) standard deviation = 0.125 MPa (White et al., 2018)

The thermal gradient surrounding the drift (Figure 5.1) was converted to a stress (σ_h) gradient of 40 kPa/m at the fracture initiation point and the resulting stress field was used to predict the geometry of the propagating fracture (Fu et al., 2018). Three sets of hydraulic fracturing simulations were executed as a: 1) coarse grid design, 2) refined model, and 3) refined model with a superimposed variation in σ_h. Details of the first and second model are described in Fu et al. (2018), with the exception of the 25-cm grid resolution used in the second model (Figure 5.4). These simulations revealed two competing factors controlling fracture geometry and evolution: 1) gradients in σ_h and 2) stress roughness caused by the rock fabric. A series of hydraulic fracturing simulations was executed using different realizations of stress heterogeneity developed from an understanding of the rock fabric (i.e., bedding planes) within the Testbed 1. Variations in the resulting predictions of fracture aperture and extent are significant with only differences in realizations of stress heterogeneity.

(a) (b)
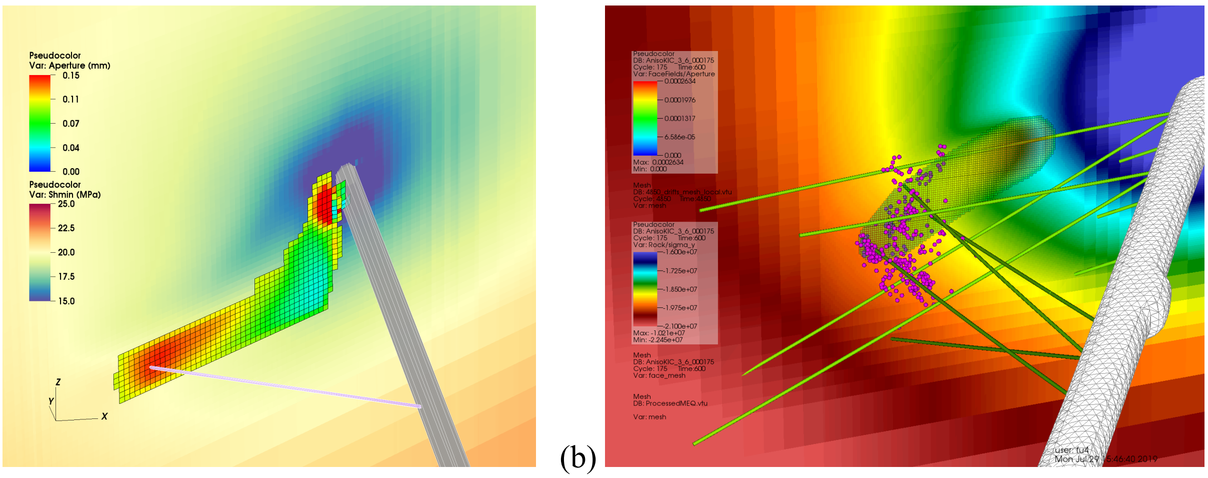

Figure 5.4: A) Fracture extents and aperture distribution after 6 minutes of injection at 0.1 L/s under the strong influence of the stress perturbation caused by the drift. Shown in the background is the magnitude of the minimum principal stress in the rock body on a planar "slice" that is parallel to and 5 m away from the expected fracture plane. The locations of the drift and the planned stimulation well are shown in the figure. B) repeated simulation with a refined grid using 25 cm resolution.

5.2.2 Hydraulic stimulation within a fractured domain

A series of simulations was executed to model the development of the fracture network initiated from the 164' Notch in E1-I (Lu and Ghassemi, 2019). The principal objective of these simulations was to compare the injection pressure profiles and induced seismicity against the field observations. A semi-deterministic fracture network consisting of 112 major fractures was developed by combining fracture image logging and core data with fracture properties that followed a stochastic distribution. A fracture within this network at the 164' Notch was considered as the primary conduit from the injection borehole. The simulations considered fracture aperture dilation, fracture slipping and fracture extension. Integration between the coupled finite element model and the semi-deterministic fracture network model was achieved by linking permeability change with fracture deformation (e.g., dilation and propagation). A stress dependent fracture deformation model with a shear dilation model was utilized to account for shear dilation. An analytic approach for fracture propagation was applied using the maximum tensile stress criterion. The induced seismicity during the injection process was also evaluated. A seismic model was developed which allowed for multiple seismic events to occur on and around a fracture. Two conditions were imposed to constrain the number of events. The switching conditions between aseismic slip and seismic slip were also resolved. One key note from this series of simulations is that the flow path from the injector to producer was dominated by a limited number of fractures, and only 4 of the 112 fractures experienced dilation during the stimulation (Figure 5.5). Fracture I-164 propagated during the stimulation period, increasing from a radius of 5 m to 6.8 m, but no wing cracks formed. Four fractures were computed to have slipped, and MEQs were computed for the slip events. The number of simulated and field-observed MEQs were 231 and 202, respectively, indicating good agreement. The locations of the simulated MEQs only matched some of the field-observed MEQs in this zone because the semi-deterministic fracture network may not reflect the actual rock mass condition (Figure 5.6).

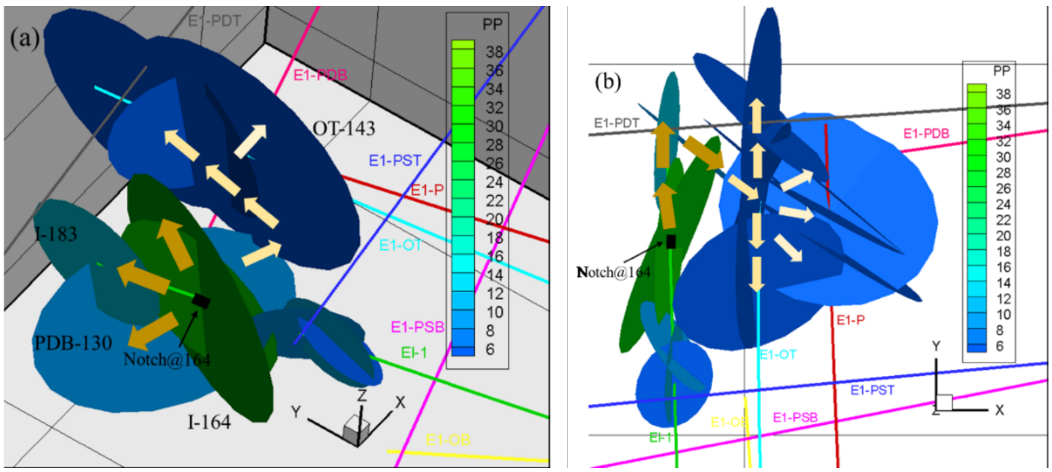

Figure 5.5: Flow path created during stimulation via water injection. The injection point is located at the 164' Notch. Fractures I-164, PDB-130, and I-183 are the major contributors to fluid circulation (fractures are name by connecting borehole and depth). Fracture PDB-130 is slightly connected to OT-143 with small volumetric flow rates crossing OT-143. The flow rates across fractures E1-OT and E1-P were computed to be low.

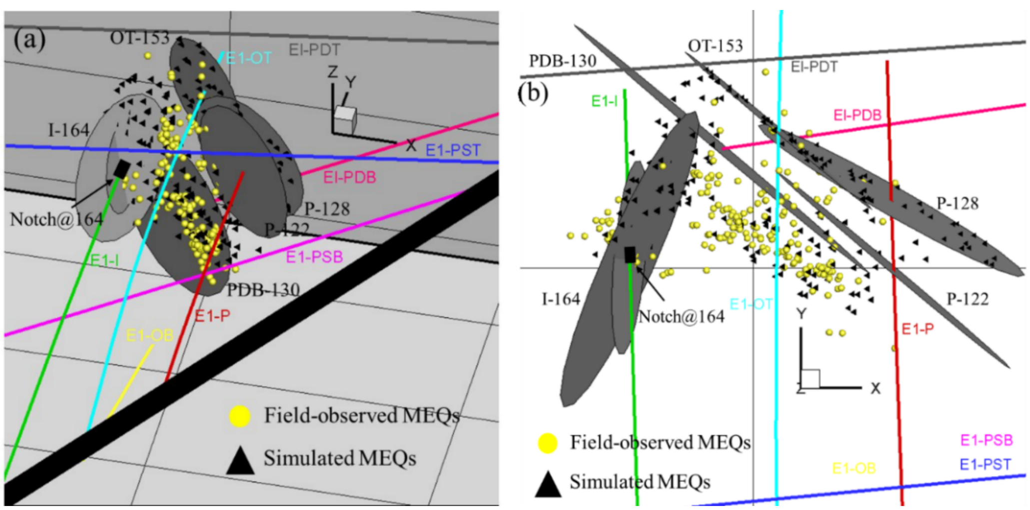

Figure 5.6: Comparison between simulated and field-observed MEQs for the hydraulic stimulation at the 164' Notch.

A subsequent series of numerical simulations was executed with natural fractures that are allowed to pressurize and slip upon coalescence with the propagating hydraulic fracture. These simulations also helped predict the injection pressure history, MEQ cloud, and fracture network evolution involving both hydraulic and natural fractures. These simulations included two sets of natural fractures situated on either side of E1-I borehole, with each having different dips, inclination angles and sizes. Simulations included the possibility for propagated wings for the natural fractures (Figure 5.7).

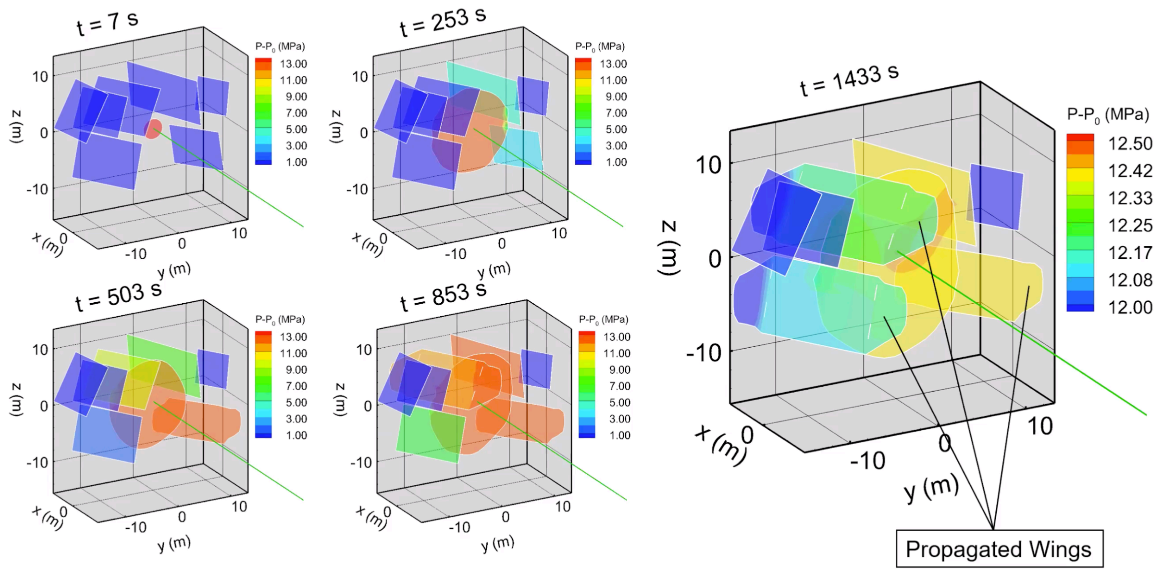

Figure 5.7: Simulation of hydraulic fracture propagation with coalescence with natural fractures from the notch at 164 ft in E1-I.

5.3 Numerical Simulations to Provide Understandings of Observed Behaviors

Results from the EGS Collab Experiment 1 were observed in real time by groups of researchers from national laboratories, universities, industry, and the GTO. Unexpected observations were often discussed in real time during the experimental broadcasts with the basis for explanations being conceptual models of complex coupled processes. Near-real time simulations were conducted regularly by leveraging high-quality baseline models to comprehend the field observations as well as to optimize testing protocol. To facilitate rapid model building at FORGE with a goal of near real-time analysis, all models created for use on the FORGE project including the grid files should be made available for use by other modelers, perhaps by means of a clearinghouse.

Numerical simulations were performed to resolve the understanding of a number of experimental observations from Experiment 1 (e.g., Zhang et al., 2018; White et al., 2019; White and Fu, 2020). Two examples are described below. The first; to understand the temperature increase noted in the monitoring boreholes at fracture intersections, and the second to understand the perceived discrepancy between rapid tracer breakthrough and nearly non-existent thermal breakthrough.

5.3.1 Joule-Thomson heating with pressure drop

A continuous length of DTS fiber was installed and grouted into the monitoring boreholes in the Testbed 1 to monitor changes in temperature throughout the long-term chilled-water test. During the stimulation at the 164’ Notch and long-term chilled-water test, a positive temperature anomaly was noted in the DTS signal within E1-OT and E1-PDT (Figure 5.8). Clearly the temperature anomaly indicated hydraulic communication between the borehole and fracture network, but the unexpected nature of it was that the temperature increased from the initial state. To forecast the time for thermal breakthrough in Experiment 1, a series of simulations were executed (Zhang et al., 2018). These simulations considered flow across a single fracture connecting an injection and production borehole, and a temperature increase was noted around the production borehole. These simulations were executed prior to the field observation of temperature increases in the monitoring boreholes, so there was no immediate project experimental evidence to support the simulation results of a temperature increase with decreasing pressure. To understand this simulation observation, a simple simulation was executed in a horizontal one-dimensional domain. The results showed a linear change (increase) in temperature against a linear decrease in pressure with a differential of dT/dP = -0.2176 ˚C/MPa, which is equivalent to the Joule-Thomson coefficient for water at 30˚C and pressures from 14 to 19 MPa. This simple series of simulations provided a potential explanation of the temperature anomalies in E1-OT and E1-PDT (i.e., pressure drop between an intersecting fracture and the borehole). Other potential explanations include water from deeper and hotter regions surrounding the experimental testbed entering the two monitoring boreholes.

5.3.2 Tracer and thermal injection tests

Although injection flow rate, pressure, and water recovery rate provide important information on the Experiment 1 testbed performance, chemical tracers provide additional information such as changes in the fracture system between the injection and production wells. Rhodamine-B, fluorescein, C-dot, and phenyl acetate were used as fluorescing tracers whereas Cl, Br, and K were used as ionic tracers (Mattson et al., 2019). These tracers in different combinations were used to evaluate the fracture pathways changes during injection purge testing, cold water injection, and chemical manipulation of the injection water. Synthetic deoxyribose nucleic acid (DNA) tracers were included during the early tracer works; however, their use was subsequently discontinued because of poor recovery.

All tracer cocktail solutions injected into the testbed included at least one fluorescing tracer for near-real time detection in the drift allowing test decision-making during field operations. The ability to detect tracer in the drift not only provided real-time analysis of the tracer breakthrough data at multiple producers but also helped modify sampling strategy (e.g., set/change sampling frequency, preference for overnight sampling) as well as modifying the experiment operation in real-time.

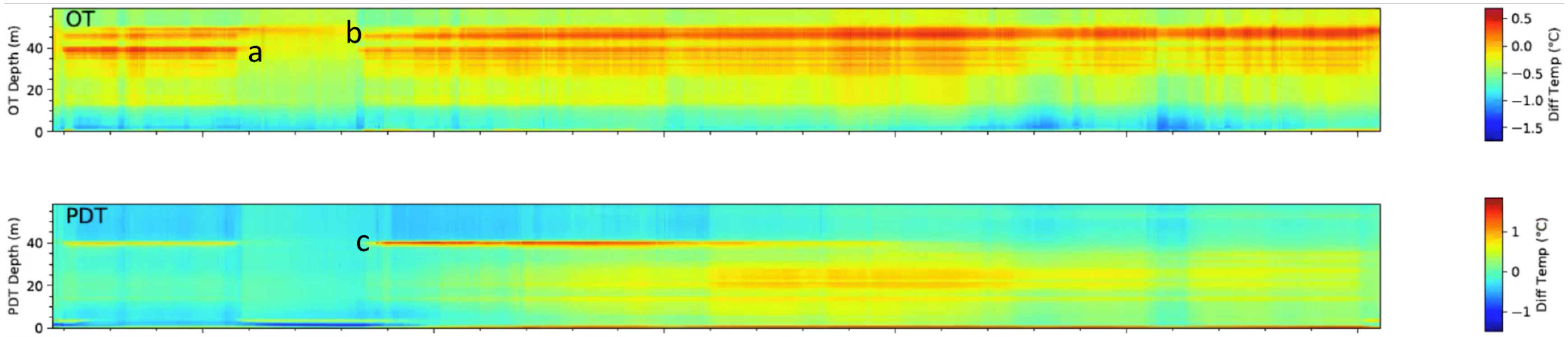

Figure 5.8: Distributed temperature sensor temperature differentials in E1-OT and E1-PDT over the period from 04/01/2019 to 06/01/2019, showing bands (as indicated by markers "a" and "c") of higher temperature near the 40 m depth in both boreholes, and 45 m depth in E1-OT (as indicated by marker "b") during periods of active flow. Each vertical line of DTS data show temperatures from the drift wall (lowest part of the panel – blue) to the deepest (top, red). Repeated measurements allow for the apparent continuous plot over time.

Over the period from 10/24/2018 through 02/03/2020 a total of 21 tracer tests were conducted, using DNAs, C-dots, rhodamine-B, fluorescein, phenyl acetate, and soluble salts (Mattson et al., 2019; Neupane et al., 2020; Mattson et al., 2021). In general, total tracer recoveries in terms of mass balance were in the 30% range, while volumetric water recoveries generally increased over time to nearly 98% by the conclusion of the long-term chilled-water test. For the C-dots arrival times for peak concentrations in PI (outflow from production hole interval) varied between 1.4 and 6.9 hours and in PB (outflow from production hole below lower packer) varied between 0.8 and 5.7 hours during the long-term chilled-water test. This result is in sharp contrast to the near negligible change in temperature measured over the course of the many months long-term chilled-water test.

A series of simulations were executed by researchers at multiple institutions to understand the contrast in tracer and thermal breakthroughs observed in the long-term chilled-water test (Wang et al., 2018; Zhou et al., 2018; Winterfeld et al., 2019; Wu et al., 2019a; Wu et al., 2019b; White et al., 2020; Beckers et al., 2020; Makedonska et al., 2020; Jafarov et al., 2020; Wu et al., 2020, Wu et al., 2021). The general finding from all of these studies was that the relatively high thermal conductivity of the phyllite could result in little thermal breakthrough. Additionally, a significant portion of the fracture is available for heat transfer and there is no evidence of extreme short circuiting under the applied conditions. However, the possibility that the recovered fluid was diluted by other formation waters cannot be eliminated, implying that while we achieved close to a 90 percent fluid balance (our volumetric fluid recovery was approximately the same as our injection), the system was not closed (Zhang et al., 2020).

5.4 Remaining Modeling Challenges

Numerical simulation is an essential component of the Collab project in two respects. First numerical simulation is contributing to the design of the meso-scale experiments that will be conducted under in-situ stress conditions and crystalline rock formations. Second the experimental measurements will serve as benchmarks against which to compare post-experimental numerical simulations. Heterogeneities in the rock fabric, natural fractures, spatial variations of in-situ stress, and other geologic features generally preclude numerical simulation from providing accurate matches to experimental outcomes. The true value of numerical simulation then comes from the understanding it provides concerning complex system behavior, allowing scientists and engineers to make informed choices about experimental designs and interpreting experimental observations. The modeling research scientists and engineers involved in the project were successful in providing experimental design guidance and understanding of experimental observations, but not all experimental observations have been addressed.

Multiple hydraulic characterization campaigns as well as long-term thermal injections were conducted in the Testbed 1. During these tests, pressure evolution during cycles of injection appeared to be informative of poroelastic and thermal processes away from the well. Even with no change in rock or the fracture network, changing temperature alters fluid density and viscosity, and thus has the potential to alter the pressure response. During many of the constant (0.4 L/min) injection cycles, injection pressure increased as the injection continued. During some of these cycles, the injection pressure buildup was particularly rapid, and was mostly remedied by a very brief shut-in followed by rapid return to original flow rates. There was some evidence that the choice of injection fluid (mine water, deionized water, softened water) had some influence on this behavior. Biofouling was observed in the water system upstream of the pump, leading to some suspicion that this was responsible for building up of the injection pressure, and slugs of biocide did appear to have an effect of halting this trend at times. Another hypothesis of this building up of injection pressure was precipitation of minerals in near wellbore fractures. Indeed dark-colored precipitates rich in carbonate minerals were recovered from equipment upon removal from the injection borehole. However, the gradual building up of pressure became less of an issue after a redesign of the pumping system that eliminated the need for a water tank that was open to the air.

Temperature measurements were not always reliable or representative of the state of the fluid at the point of injection into the formation. Specifically, the temperature of water entering a borehole might be known, but not that as it enters the fracture. Consequently, to better understand thermal effects on the formation, flow in the borehole itself needed to be modelled, when it would have been best to measure relevant fluid temperatures directly.

Understanding the interplay between chemistry, biology, poroelastic and thermal processes is key to interpreting injection-pressure data. The rates at which chemistry may impact flow can be surprisingly fast, complicating the injectivity data interpretation. Water chemistry and its interactions with the engineered systems and the formation need to be understood. Even with the sophisticated measurement techniques available, it may not be possible to know boundary conditions on the scale that mechanistic models may require. Thus, a disconnect must often be accepted between actual and model boundaries. Reducing the severity of this disconnect may be necessary for determining which process creates the difference between observed and modeled results. When clever models are created to overcome these disconnects, the modeling tools should be collected and made available to other FORGE researchers, perhaps by means of a clearinghouse.

This section describes three potential targets for future modelling efforts related to pressure response to injection of various types of waters (e.g., mine water, low EC water, chilled water, etc.) for Experiment 1.

5.4.1 Increased Flow Resistance with the Injection of Non-Chilled Water

The long-term chilled-water test was originally planned to be preceded with a period of un-chilled water injection. The minimum horizontal stress in the testbed was estimated to be 21.7 MPa (3147 psi) and the maximum horizontal stress in the testbed was estimated to be 35.5 MPa (5148 psi), and reopening pressure was not anticipated to be significantly higher than the minimum horizontal stress, but as shown in period "a" injection temperature and pressure plot (Figure 5.9), the injection pressure at a constant injection rate of 0.4 L/min steadily increased. To investigate whether chilled water would alter this increasing injection pressure, the chilled water (12.1˚C) injection was started with a nearly immediate associated drop in injection pressure from 4580 psi (31.58 MPa) to 4225 psi (29.13 MPa). The injection-water chillers remained on throughout the remainder of the long-term chilled-water test, except for short periods of time for operational issues (e.g., chiller maintenance, power outage, etc.). During each of these types of events, noted as "b", "c", and "d" in Figure 5.9, there was an associated increase in the injection pressure with an increase in the temperature of the injection water. This observation suggests a near borehole thermo-mechanical process controlling the flow resistance. This could be modelled as a temperature-dependent wellbore skin factor, but that approach does not provide any insight to the mechanism behind the observation. One intriguing aspect of this behavior is the near immediate response in pressure drop with the resumption of chilled water injection.

5.4.2 Increased Flow Resistance over the Course of Experiment 1

The previous section described the observed pressure drop associated with the injection of chilled water, but the long-term chilled-water test additionally had a slowly increasing injection pressure over the course of the test (Figure 5.9). A hypothesis has emerged to explain the steady rise of injection pressure during the longer-term injections, which appeared consistent with poroelastic effects. This pressure rise could also indicate a gradual filling of a fracture network within a quasi-closed volume of rock thereby increasing the local matrix pore pressure and resulting in increased normal stress on the fractures and a reduced aperture. Reduced fracture aperture yields increased flow resistance, which at a constant injection rate, results in increased injection pressures, matching the experimental observation. One indication of this is the reduced overall leakoff over time as indicated by the increase in volumetric water recoveries during the test. Increasing injection pressure over time could lead to pressures that exceeded the propagation pressure, which was not desirable for the project such that the continuous propagation of the fracture to the drift would have halted the experiment. Simulations designed to understand this gradual increase in flow resistance over time would be beneficial to understanding Experiment 1, but more generally the coupled mechanisms of EGS fracture networks.

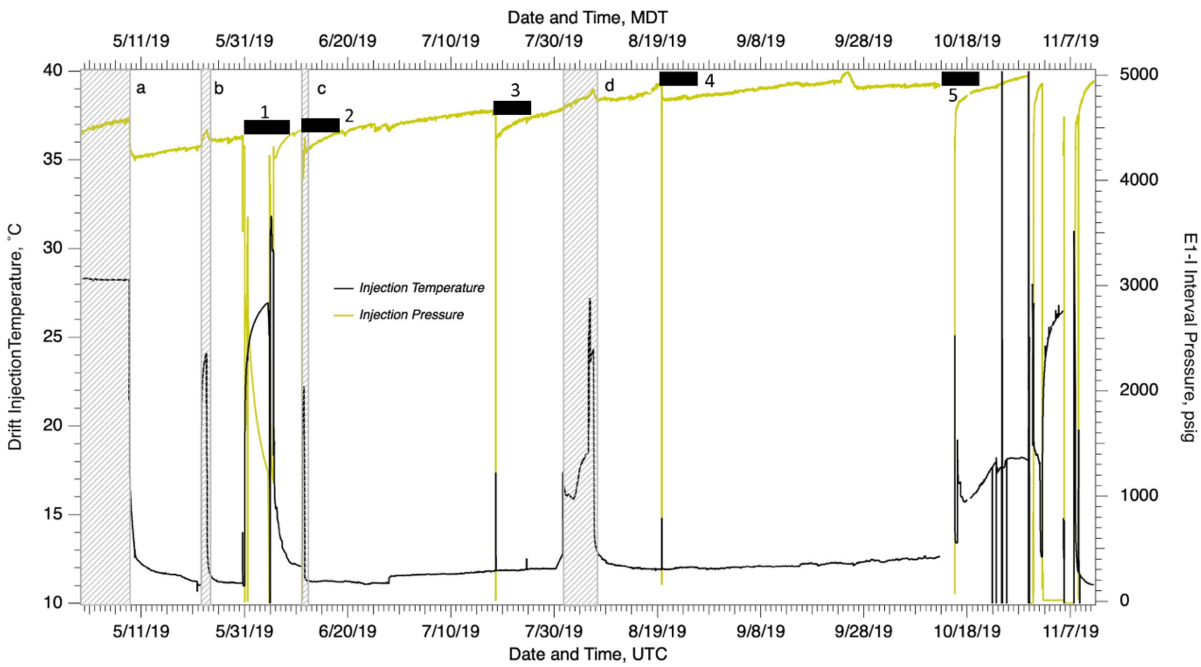

Figure 5.9: Temperature of the water injected at the borehole collar versus time against the E1-I interval pressure. The markers "a" through "d" represent the period of interruptions in operation of chiller, and the markers "1" through "5" represent the interruptions in pumping and interval pressure response upon resumptions of pumping.

5.4.3 Decreased Flow Resistance with Halts in Chilled-Water Injection

The long-term chilled-water test achieved its principal objective of a long-term circulation experiment, but it was not without occasional interruptions in pumping (Figure 5.10). These interruptions, as noted "1" through "5" in Figure 5.9, lasted from minutes to about a week. Regardless of the length of interruptions, resumption of chilled-water injection at the original pumping rate of 0.4 L/min occurred at reduced pressure in the injection interval. The injection interruption indicated by "1" lasted about a week. For this longer interruption, the decrease in injection pressure after resumption of pumping could have resulted by reductions in the matrix pore pressure resulting of drainage which in turn caused an increased normal stress on the fracture surfaces. However, other interruptions were for too short period to have yielded a significant pressure decay in the matrix pore pressure yet resulted in a reduction in injection pressure – in other words, a reduction in flow resistance across the fracture network, for a constant pumping rate. It is important to note that after each injection pumping stoppage and associated injection pressure decrease, the injection pressure returns to the pre-stoppage level after some period of time, and continues to gradually rise. This drop in flow resistance after the briefest of stoppage in flow is intriguing, and remains to be understood.

5.5 Lessons Learned

Initial numerical simulations of the stimulation of a hydraulic fracture within the Experiment 1 testbed forecasted a penny-shaped fracture with seismic magnitudes of 0.1 on the Richter scale. Inclusion of information about the stress state being altered by drift cooling and rock fabric yielded very different shaped hydraulic fractures, elongated in shape with little to no extension on the side opposite the production borehole. The later numerical simulations were executed in response, however, to the observed MEQ event locations. The current understanding of the fracture network in the Testbed 1 is one with two hydraulic fractures emanating from the injection borehole near the notch at 164 ft, intersecting the OT-P connector natural fracture, and then proceeding past the production borehole as two distinct fracture wings (Figure 5.10). Two conclusions can be drawn about using numerical simulation to constrain active flow paths in the testbed. First, the fracture network evolved over an iterative process of simulation, characterization, and experimental observation. Second, comparing the most recent numerical simulations of the development of the fracture network (Figure 5.6) against the current understanding of the fracture network, there remain differences.

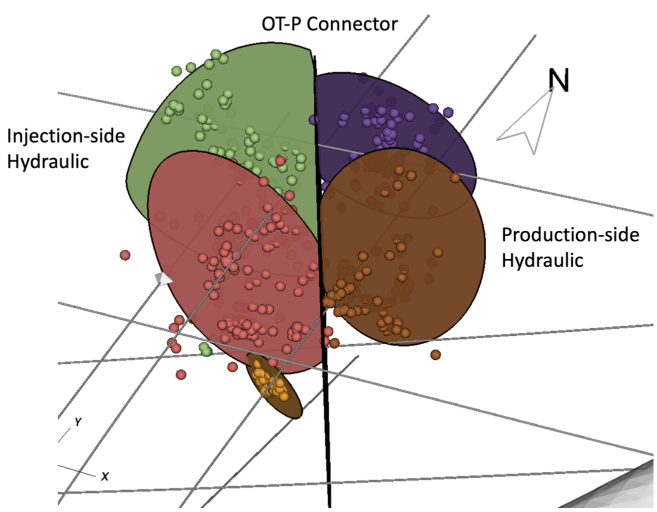

Figure 5.10: Dominant hydraulic and natural fractures of Experiment 1.

The common discrete fracture network developed for the Testbed 1 contains a large number of fractures (Figure 1.3). However, a limited number of conductive fractures dominated the flow paths, and this number seemed to decrease over time during the experiment. The weep zones which initially contributed to water recovery on the drift wall either declined or stopped flowing over the course of the experiment. Numerical simulations of tracer and thermal recovery were able to reproduce the experimental observations using a small number of dominant fractures that were aligned with the seismic event locations.

The tests and experiments that will occur at FORGE will result in numerous observations and many of these may be difficult to explain. Identifying processes that could result in these observations will require appropriate models, good simulators, and knowledgeable modelers willing to consider all possible solutions. Applying simulation tools used in Collab to FORGE or other projects with elevated temperatures will require stepwise confidence-building in the hands of experienced modelers knowledgeable of the processes occurring. If this is performed, the process is likely to be successful. Specifically, thermomechanical, poroelastic, and geochemical changes will occur at different rates than at Collab. Higher temperature will strongly affect geochemistry including dissolution and precipitation. Temperature gradients are likely to be much higher at FORGE, more strongly affecting thermomechanical behavior. Rock properties may also vary over the strong gradient, and the ability to simulate *all* of these processes will be needed. An advantage at FORGE is the ability to drive the system harder and over a larger range of flows and temperatures than at Collab. These factors will be helpful in determining the relative contribution of processes to the observed behavior.

6. Summary and Concluding Remarks

Collab is performing experiments utilizing readily accessible underground facilities to refine understanding of rock mass response to stimulation using intermediate scale (on the order of 10 m) under EGS-relevant stress conditions. The project focuses on understanding and predicting permeability enhancement and evolution in crystalline rock, including how to create sustained and distributed permeability for heat extraction from a reservoir by generating new fractures that complement existing natural fractures. Results from stimulation, flow, tracer, and thermal tests are being used to validate coupled THMC modeling approaches applicable to EGS. Collab is also testing and improving conventional and novel field monitoring tools. FORGE has the mission of establishing an EGS field test site that enables cutting-edge research and testing for EGS technology, as well as allowing scientists to identify a replicable, commercial pathway to EGS.

The most relevant lessons in 1) data processing, annotation, and integration; 2) processing seismic data, 3) connecting geophysics, fractures, and flow systems, and 4) challenges of modeling fractured flow systems have been presented. Conclusions include:

Data processing, annotation, and integration

Data management was addressed at the outset of the project by implementing a data management plan that was designed by data experts working together with data generators and data users. This has allowed effective use, transfer, and distribution of the large quantity of data that has been generated and collected during Collab Experiment 1. The most valuable system for data handling is the Data Foundry. Streaming live data collection to the Data Foundry allowed rapid sharing. Rapid organization, annotating, and presenting many streams of data in a readily understood manner *as soon as possible* enabled informed engineering decisions, and described data for future in depth analysis. Making experimental data accessible to a broad community helped both expand the perspectives to scientific and engineering interpretations as well as make many important discoveries. Temporal and/or spatial synchronization of multi-faceted data sets was found to reveal processes that may be obscured in individual measurements, and/or corroborate other data streams allowing for more definitive conclusions.

Processing seismic data

Key subsets of the Collab data are the active and passive seismic data from an intensively equipped seismic monitoring system. The large number of sensors and their deployment in a 3D distribution around the stimulation zone via the 6 monitoring wells enabled rapid high-quality hypocenter determination with likely spatial resolution at the sub-meter level. The high sensitivity of the accelerometer pods used allowed for production of a large event catalog. Machine learning algorithms were used to refine the catalog, ultimately allowing precise identification of fracture planes, even those in close proximity to each other. The value of these data was increased by an edge processing framework developed within the Collab project, which allowed for near real-time event detection and location, a process which provided almost immediate feedback into field operations. Seismic data streams generated using the fiber optic sensing system (DAS) have required more intensive analysis and interpretation, which resulted in significant delays in the utilization of these data. New approaches are under development to speed up the interpretation and use of these data. These approaches could be beneficial to FORGE.

Connecting geophysics, fractures, and flow systems

Direct observation of complete cores, interpretation of image logs, fracture/shear zone mapping in the vicinity of the testbed, and a range of geophysical and hydraulic measurements including tracer tests were needed to characterize the natural as well as created hydraulic fractures and flows in the testbed. To the extent possible, all data sets were then integrated into a discrete fracture network model, which served as a basis for conceptualizing fracture flow pathways. Timely reconstruction, orienting core, and correlation to wireline measurements are needed to provide key information on the subsurface environment. Despite being able to characterize and monitor major natural and created fractures at individual levels, challenges in disentangling the thermal exchange/heat extraction of the fracture system in the testbed exist.

MEQ monitoring was the primary tool used to characterize and monitor reservoir evolution during Experiment 1. Injection flowrate, pressure, ERT, distributed fiber optic sensing (temperature - DTS, strain - DSS, and acoustic - DAS), downhole camera observations, and tracer testing were conducted during Experiment 1 as well. Tracer tests helped reveal the dynamic behavior of the test bed, where the proportions of flow through different fracture networks varied with time. This comprehensive monitoring enabled us to compare the detailed testbed behavior from multiple measurement perspectives.

Time-lapse measurements using multiple techniques including simple hydrological to geophysical methods improved the understanding of the initial system *and* changes in the system. Collected data must be processed in an appropriate timeframe to make it valuable. Joint interpretation of multiple data streams is key to providing additional understanding.

Collab used a large number of highly instrumented dedicated monitoring wells to fully surround the target zone with sensors, resulting in for example high accuracy hypocenter determination. CASSM & dynamic ERT were deployed for one of the first times in a complicated geothermal testbed to provide a broader description of processes. Similar implementation of some of these techniques may not be feasible at FORGE because of temperature and cost of application. Combined fiber optic sensing has been extremely valuable at Collab for the low relative cost and quality and quantity of data collected. These techniques are likely compatible for the operating conditions at FORGE.

Challenges of modeling fractured flow systems

In the Collab project, numerical simulations were successfully executed to 1) support experimental designs, 2) estimate the magnitudes of the effects of the applied stimuli to obtain approvals to proceed, 3) forecast outcomes of operational changes, and 4) provide understanding of observed behaviors. Validation of numerical simulation tools is a stated objective of the Collab project, with the principal objective of learning whether the capabilities of modern state-of-the-art simulators are sufficient to accurately predict stimulation, fracture networks, and subsequently thermal energy recovery for the Collab experiments.

Many model validations have been performed by comparing the results of numerous simulations to measurements. Confidence in numerical simulation was built by modelers who began with detailed understanding of the experiments in addition to having expert use of codes that incorporate known processes to the extent reasonable. Simulations performed in near-real-time yielded reliable high-quality solutions to a team that understands the value *and* limitations of the modeling efforts. It is understood that unknowable heterogeneities in the rock fabric, natural fractures, spatial variations of in-situ stress, and other geologic features generally preclude numerical simulation from providing accurate matches to experimental outcomes. Numerical simulation provided understanding of complex system behavior, allowing scientists and engineers to make informed choices about experimental designs and interpreting experimental observations.

Many challenges in simulating fracture flow and heat extraction remain. The interplay between poroelastic, thermal, chemical, and biological processes is thought to be key to interpreting injection-pressure data. Providing appropriate measured boundary conditions on the scale that a mechanistic model may require may not be possible. Modeling a dynamic system is another challenge. Appropriate observations and data are needed to determine the magnitudes of the responsible processes. The models can be used to offer insights into processes and process magnitudes, and provide a guide to the next measurements needed. Application of these simulation tools to FORGE or other sites with elevated temperatures will require additional stepwise confidence building in the hands of experienced modelers knowledgeable of the processes requiring consideration. If this is performed, the process is likely to be successful.

References

Beckers, K.F., Johnston, B., Winterfeld, P., Wu, Y.S., Neupane, G., Mattson, E.D., Hawkins, A., and EGS Collab Team, 2020. Analysis of EGS Collab tracer and thermal tests using analytical and numerical tools. In Preparation.

Caddey, S.W., Bachman, R.L., Campbell, T.J., Reid, R.R. and Otto, R.P., 1991. The Homestake gold mine, an early Proterozoic iron-formation-hosted gold deposit, Lawrence County, South Dakota. 1857J.

Carter, T.G., Carvalho, L.L., Otto, S.A., Popielak, R., Vardiman, D. and Hladysz, Z., 2011. January. Preliminary Design of the 4850-Level Excavations at DUSEL Part 1-Geological Engineering Evaluation of Rock Mass Conditions. 45th US Rock Mechanics/Geomechanics Symposium. American Rock Mechanics Association, San Francisco, California, pp. 8.

Chai, C., Maceira, M., Santos-Villalobos, H., Venkatakrishnan, S. V., Schoenball, M., Zhu, W., et al. (2020). Using a Deep Neural Network and Transfer Learning to Bridge Scales for Seismic Phase Picking. *Geophysical Research Letters*. 47(16), e2020GL088651.

Chen, Y., Huang, L. and Team, E.C., 2018. Microseismic Moment-Tensor Inversion for the EGS Collab Project: A Synthetic Study. Proceedings, 43rd Workshop on Geothermal Reservoir Engineering, Stanford, California.

Chen, Y., Huang, L. and the EGS Collab Team, 2019. Optimal design of 3D borehole seismic arrays for microearthquake monitoring in anisotropic media during stimulations in the EGS collab project. *Geothermics*, 79, 61-66.

Condon, K. J., Sone, H., Wang, H.F., 2020. Low Static Shear Modulus Along Foliation and Its Influence on the Elastic and Strength Anisotropy of Poorman Schist Rocks, Homestake Mine, South Dakota. *Rock Mechanics and Rock Engineering*, 53(11), 5257-5281.

Dobson, P., Kneafsey, T.J., Blankenship, D., Valladao, C., Morris, J., Knox, H., Schwering, P., White, M., Doe, T., Roggenthen, W., Mattson, E., Podgorney, R., Johnson, T., Ajo-Franklin, J. and EGS Collab Team, 2017. An Introduction to the EGS Collab Project. *GRC Transactions*, 41, pp. 17.

Doe, T.W., McLaren, R. and Dershowitz, W., 2014. Discrete Fracture Network Simulations of Enhanced Geothermal Systems. Proceedings, 39th Workshop on Geothermal Reservoir Engineering, Stanford, California.

Frash, L.P., Arora, K., Gan, Y., Lu, M., Gutierrez, M., Fu, P., Morris, J., Hampton, J. and EGS Collab Team, 2018a. Laboratory validation of fracture caging for hydraulic fracture control, 52nd U.S. Rock Mechanics/Geomechanics Symposium. American Rock Mechanics Association, Seattle, Washington, pp. 8.

Frash, L.P., Fu, P., Morris, J., and EGS Collab Team, 2018b. Fracture caging: can we control the extent of a hydraulic fracture stimulated zone? Proceedings, 43rd Workshop on Geothermal Reservoir Engineering, Stanford, California.

Frash, L.P., Welch, N.J., Carey, J.W., and EGS Collab Team, 2019. Geomechanical evaluation of natural shear fractures in the EGS Collab Experiment 1 test bed. 53rd US Rock Mechanics/Geomechanics Symposium. American Rock Mechanics Association, New York, NY, USA, pp. 7.

Frash, L.P., Fu, P., Morris, J., Gutierrez, M., Neupane, G., Hampton, J., Welch, N.J., Carey, J.W. and Kneafsey, T., 2020. Fracture caging to limit induced seismicity. *Geophysical Research Letters*, p.e2020GL090648.

Fu, P., Johnson, S.M. and Carrigan, C.R., 2013. An explicitly coupled hydro-geomechanical model for simulating hydraulic fracturing in arbitrary discrete fracture networks. *International Journal for Numerical and Analytical Methods in Geomechanics*, 37(14), 2278-2300.

Fu, P., White, M.D., Morris, J.P., Kneafsey, T.J. and EGS Collab Team, 2018. January. Predicting hydraulic fracture trajectory under the influence of a mine drift in EGS Collab experiment I. Proceedings, 44th Workshop on Geothermal Reservoir Engineering, Stanford, California.

Fu, P., Schoenball, M., Ajo-Franklin, J.B., Chai, C., Maceira, M., Morris, J.P., Wu, H., Knox, H., Schwering, P.C., White, M.D. Burghardt, J.A., Strickland, C.E., Johnson, T.C., Vermeul, V.C., Sprinkle, P., Roberts, B., Ulrich, C., Guglielmi, Y., Cook, P.J., Dobson, P.F., Wood, T., Frash, L.P., Huang, L., Ingraham, M.D., Pope, J.S., Smith, M.M., Neupane, G., Doe, T.W., Roggenthen, W.M., Horne, R., Singh, A., Zoback, M.D., Wang, H., Condon, K., Ghassemi, A., Chen, H., McClure, M.W., Vandine, G., Blankenship, D., Kneafsey, T.J., andEGS Collab Team, 2021. Close observation of hydraulic fracturing at EGS Collab Experiment 1: Fracture trajectory, microseismic interpretations, and the role of natural fractures. *Journal of Geophysical Research: Solid Earth*, p.e2020JB020840.

Gao, K., Huang, L., Chi, B., Ajo-Franklin, J. and the EGS Collab Team, 2018. Imaging the Fracture Zone Using Continuous Active Source Seismic Monitoring for the EGS Collab Project: A Synthetic Study. Proceedings, 43rd Workshop on Geothermal Reservoir Engineering, Stanford, California.

Guglielmi, Y., Cappa, F., Avouac, J.-P., Henry, P. and Elsworth, D., 2015. Seismicity triggered by fluid injection–induced aseismic slip. Science, 348(6240): 1224.

Guglielmi, Y., Cappa, F., Lançon, H., Janowcsyk, J. B., Rutqvist, J., Tsang, C.-F., & Wang, J. S. Y., 2014. ISRM Suggested Method for Step-Rate Injection Method for Fracture In-Situ Properties (SIMFIP): Using a 3-Components Borehole Deformation Sensor. *Rock Mechanics and Rock Engineering*, *47*(1), 303–311.

Guglielmi, Y., Cappa, F., Lançon, H., Janowczyk, J.B., Rutqvist, J., Tsang, C.F. and Wang, J.S.Y., 2013. ISRM Suggested Method for Step-Rate Injection Method for Fracture In-Situ Properties (SIMFIP): Using a 3-Components Borehole Deformation Sensor. In: R. Ulusay (Editor), The ISRM Suggested Methods for Rock Characterization, Testing and Monitoring: 2007–2014. Springer-Verlag, Wein.

Guglielmi, Y., P. Cook, P., Soom, F., Schoenball, M., Dobson, P., and Kneafsey, T., 2021. In situ continuous monitoring of borehole displacements induced by stimulated hydrofracture growth. *Geophysical Research Letters, 48, e2020GL090782*.

Hart, K., Trancynger, T.C., Roggenthen, W. and Heise, J., 2014. Topographic, geologic, and density distribution modeling in support of physics experiments at the Sanford Underground Research Facility (SURF). Proceedings of the South Dakota Academy of Science, 93: 33-41.

Heise, J., 2015. The Sanford Underground Research Facility at Homestake. *Journal of Physics: Conference Series*, 606(1): 26.

Huang, H., Zhou, J., Mattson, E. and Podgorney, R., 2018. Mechanistically modeling of hydraulic fracture opening, closure and residual fracture permeability during cyclic flow injection tests. *GRC Transactions*, 42, p. 11.

Huang, H., G. H. Neupane, R. Podgorney, E. Mattson, and the EGS Collab Team (2019), Mechanistically Modeling of Hydraulic Fracture Propagation and Interaction with Natural Fractures at EGS-Collab Site paper presented at 44th Workshop on Geothermal Reservoir Engineering, Stanford University, Stanford, California, February 11-13, 2019.

Huang, L., Chen, Y., Gao, K., Fu, P., Morris, J., Ajo-Franklin, J., Nakagawa, S. and EGS Collab Team, 2017. Numerical Modeling of Seismic and Displacement-Based Monitoring for the EGS Collab Project. *GRC Transactions*, 41, 893-909.

Jafarov, E.E., Makedonska, N., Karra, S., Pawar, R., Beisman, J., Neupane, G., Schwering, P.C., Kneafsey, T.J. and EGS Collab Team, 2020. Simulations of the 3D Geothermal Heat Flow in Fractured Media. Proceedings, 45th Workshop on Geothermal Reservoir Engineering, Stanford, California.

Johnson, T. C., Strickland, C., Vermeul, V., Mattson, E., Knox, H. A., Ajo-Franklin, J., et al. (2019). EGS Collab Project Electrical Resistivity Tomography Characterization and Monitoring. Proceedings 44th Workshop on Geothermal Reservoir Engineering, Stanford California.

Johnson, T., C., Versteeg, R., J., Day-Lewis, F., D., Major, W. and W., L.J., 2014. Time-Lapse Electrical Geophysical Monitoring of Amendment-Based Biostimulation. *Groundwater*, 53(6), 920-932.

Klein, F.W., 2014. User's Guide to HYPOINVERSE-2000, a Fortran Program to Solve for Earthquake Locations and Magnitude. U.S. Geological Survey, Open File Report 02-171.

Kneafsey, T. J., Blankenship, D., Knox, H. A., Johnson, T. C., Ajo-Franklin, J., Schwering, P. C., et al. (2019a). EGS Collab Project: Status and Progress. Proceedings, 44th Workshop on Geothermal Reservoir Engineering, Stanford, California.

Kneafsey, T.J., Blankenship, D., Dobson, P.F., Morris, J.P., White, M.D., Fu, P., Schwering, P.C., Ajo-Franklin, J.B., Huang, L., Schoenball, M., Johnson, T.C., Knox, H.A., Neupane, G., Weers, J., Horne, R., Zhang, Y., Roggenthen, W., Doe, T., Mattson, E., Valladao, C. and EGS Collab Team, 2020a. The EGS Collab Project: Learnings from Experiment 1. Proceedings, 45th Workshop on Geothermal Reservoir Engineering, Stanford, California.

Kneafsey, T.J., Dobson, P., Blankenship, D., Morris, J., Knox, H., Schwering, P., White, M., Doe, T., Roggenthen, W., Mattson, E., Podgorney, R., Johnson, T., Ajo-Franklin, J., Valladao, C. and EGS Collab Team, 2018. An Overview of the EGS Collab Project: Field Validation of Coupled Process Modeling of Fracturing and Fluid Flow at the Sanford Underground Research Facility, Lead, SD. Proceedings 43rd Workshop on Geothermal Reservoir Engineering, Stanford, California.

Kneafsey, T.J., P.F., D., Ajo-Franklin, J.B., Guglielmi, Y., Valladao, C.A., Blankenship, D.A., Schwering, P.C., Knox, H.A., White, M.D., Johnson, T.C., Strickland, C.E., Vermuel, V.R., Morris, J.P., Fu, P., Mattson, E., Neupane, G.H., Podgorney, R.K., Doe, T.W., Huang, L., Frash, L.P., Ghassemi, A., Roggenthen, W. and EGS Collab Team, 2019b. EGS Collab Project: Status, Tests, and Data, 53rd US Rock Mechanics/Geomechanics Symposium, New York, NY, USA, pp. 19.

Kneafsey, T. and EGS Collab Team, 2020b. The EGS Collab Project: An intermediate-scale field test to address enhanced geothermal system challenges. In E3S Web of Conferences, 205, 01002.

Knox, H., Fu, P., Morris, J., Guglielmi, Y., Vermeul, V., Ajo-Franklin, J., Strickland, C., Johnson, T., Cook, P., Herrick, C., Lee, M. and EGS Collab Team, 2017. Fracture and Flow Designs for the Collab/Sigma-V Project. *GRC Transactions*, Vol. 41, 2017

Knox, H.A., Ajo-Franklin, J., Johnson, T.C., Morris, J.P., Grubelich, M.C., Preston, L.A., , Knox, J.M. and King, D., 2016. High energy stimulations imaged with geophysical change detection techniques. *GRC Transactions*, pp. 11.

Krischer, L., Megies, T., Barsch, R., Beyreuther, M., Lecocq, T., Caudron, C., & Wassermann, J. (2015). ObsPy: a bridge for seismology into the scientific Python ecosystem. *Computational Science & Discovery*, *8*(1), 014003.

Kutun, K., Miskimins, J.L. and Beckers, K.F., 2018, August. Hydraulic fracture modeling in support of EGS collab treatment designs. Hydraulic fracture modeling in support of EGS Collab treatment designs. 52nd U.S. Rock Mechanics/Geomechanics Symposium, American Rock Mechanics Association, Seattle, Washington.

Kwiatek, G., Martínez-Garzón, P., Plenkers, K., Leonhardt, M., Zang, A., von Specht, S., et al. (2018). Insights Into Complex Subdecimeter Fracturing Processes Occurring During a Water Injection Experiment at Depth in Äspö Hard Rock Laboratory, Sweden. *Journal of Geophysical Research: Solid Earth*, *123*, 6616–6635.

Kwiatek, G., Plenkers, K., & Dresen, G., 2011. Source parameters of picoseismicity recorded at Mponeng Deep Gold Mine, South Africa : Implications for Scaling Relations. *Bulletin of the Seismological Society of America*, *101*(6), 2592–2608.

Li, Z., D. Elsworth, C. Wang, L. Boyd, Z. Frone, E. Metcalfe, et al. and the E. G. S. Collab Team (2021), Constraining maximum event magnitude during injection-triggered seismicity, *Nature Communications*, *12*(1), 1528, doi:10.1038/s41467-020-20700-4.

Linneman, D., Knox, H., Schwering, P. and Hoots, C.R., 2018. The EGS Collab Hydrofracture Experiment at the Sanford Underground Research Facility – Campaign Cross-Borehole Seismic Characterization, H11Q-1689, AGU Fall Meeting, Washington, D.C.

Makedonska, N., Jafarov, E., Doe, T., Schwering, P., Neupane, G. and EGS Collab Team, 2020. Simulation of injected flow pathways in geothermal fractured reservoir using discrete fracture network model. Proceedings, 45th Workshop on Geothermal Reservoir Engineering, Stanford, California.

Mattson, E., Zhang, Y., Hawkins, A., Johnson, T., Ajo-Franklin, J., Neupane, G. and the EGS Collab Team, 2019. Preliminary Collab Fracture Characterization Results from Flow and Tracer Testing Efforts. Proceedings 44th Workshop on Geothermal Reservoir Engineering, Stanford, California.

Mattson, E.D., Neupane, G., White, M.D., Ingraham, M.D., and EGS Collab Team, 2021. EGS-Collab Experiment 1 Flow and Tracer Tests at the Stanford Underground Research Facility. , 55th US Rock Mechanics/Geomechanics Symposium, Houston, TX, USA, pp. 8.

Meng, M., Frash, L.P., Li, W., Welch, N.J., Carey, J.W., Ulrich, C. and Kneafsey, T.J., 2021. Hydro-mechanical measurements and x-ray imaging of sheared crystalline rock fractures from EGS Collab experiments 1 & 2. https://doi.org/10.1002/essoar.10506859.1

Moore, J., McLennan, J., Allis, R., Pankow, K., Simmons, S., Podgorney, R., Wannamaker, P., Bartley, J., Jones, C. and Rickard, W., 2019. The Utah Frontier Observatory for Research in Geothermal Energy (FORGE): An International Laboratory for Enhanced Geothermal System Technology Development. Proceedings 44th Workshop on Geothermal Reservoir Engineering, Stanford, California.

Morris, J.P., Dobson, P., Knox, H.A., Ajo-Franklin, J., White, M.D., Fu, P., Burghardt, Kneafsey, T.J., Blankenship, D., and EGS Collab Team, 2018. Experimental Design for Hydrofracturing and Fluid Flow at the DOE EGS Collab Testbed. Proceedings, 43rd Workshop on Geothermal Reservoir Engineering, Stanford, California.

Nielson, D.L., Evans, S.H., and Sibbett, B.S, 1986. Magmatic, structural, and hydrothermal evolution of the Mineral Mountains intrusive complex Utah. *Geological Society of America Bulletin*, 97, 765-777.

Neupane, G., Mattson, E.D., Plummer, M.A., Podgorney, R.K. and EGS Collab Team, t., 2020. Results of Multiple Tracer Injections into Fractures in the EGS Collab Testbed-1. Proceedings, 45th Workshop on Geothermal Reservoir Engineering, Stanford, California.

Neupane, G., Podgorney, R.K., Huang, H., Mattson, E.D., Kneafsey, T.J., Dobson, P.F., Schoenball, M., Ajo-Franklin, J.B., Ulrich, C., Schwering, P.C., Knox, H.A., Blankenship, D.A., Johnson, T.C., Strickland, C.E., Vermeul, V.R., White, M.D., Roggenthen, W., Uzunlar, N., Doe, T.W. and Team, T.E.C., 2019. EGS Collab Earth Modeling: Integrated 3D Model of the Testbed. *GRC Transactions*, 43: 21.

Newman, G. and Petrov, P., 2018. Seismic Source Mechanism Estimation in 3D Elastic Media, Proceedings, 43rd Workshop on Geothermal Reservoir Engineering, Stanford, California.

Oldenburg, C.M., Dobson, P.F., Wu, Y., Cook, P.J., Kneafsey, T.J., Nakagawa, S., Ulrich, C., Siler, D.L., Guglielmi, Y., Ajo-Franklin, J., Rutqvist, J., Daley, T.M., Birkholzer, J.T., Wang, H.F., Lord, N.E., Haimson, B.C., Sone, H., Vigilante, P., Roggenthen, W.M., Doe, T.W., Lee, M.Y., Ingraham, M., Huang, H., Mattson, E.D., Zhou, J., Johnson, T.J., Zoback, M.D., Morris, J.P., White, J.A., Johnson, P.A., Coblentz, D.D. and Heise, J., 2017. Hydraulic fracturing experiments at 1500 m depth in a deep mine: Highlights from the kISMET project. Proceedings, 42nd Workshop on Geothermal Reservoir Engineering, Stanford, California.

Roggenthen, W.M. and Koch, C.D., 2013. January. Geophysical logging of DUSEL core and geotechnical applications. In 47th US Rock Mechanics/Geomechanics Symposium. American Rock Mechanics Association, San Francisco, California, pp. 8.

Roggenthen, W.M. and Doe, T.W., 2018. Natural Fractures and Their Relationship to the EGS Collab Project in the Underground of the Sanford Underground Research Facility (SURF), 52nd U.S. Rock Mechanics/Geomechanics Symposium. American Rock Mechanics Association, Seattle, Washington, pp. 11.

Schoenball, M., Ajo-Franklin, J., Blankenship, D., Cook, P., Dobson, P., Guglielmi, Y., Fu, P., Kneafsey, T., Knox, H., Petrov, P., Robertson, M., Schwering, P., Templeton, D., Ulrich, C., Wood, T. and the EGS Collab Team, 2019a. Microseismic monitoring of meso-scale stimulations for the DOE EGS Collab project at the Sanford Underground Research Facility. Proceedings, 44th Workshop on Geothermal Reservoir Engineering, Stanford, California.

Schoenball, M., Ajo-Franklin, J. B., Robertson, M., Wood, T., Blankenship, D., Cook, P., Dobson, P., Guglielmi, Y., Fu, P., Kneafsey, T., Knox, H., Petrov, P., Schwering, P., Templeton, D., Ulrich, C., Li, J., Chi, B., Hopp, C., and the EGS Collab Team, 2019b. *EGS* Collab Experiment 1: Microseismic Monitoring. GDR Submission # 1166, https://doi.org/10.15121/1557417.

Schoenball, M., Ajo-Franklin, J.B., Blankenship, D., Chai, C., Chakravarty, A., Dobson, P., Hopp, C., Kneafsey, T., Knox, H.A., Maceira, M. and Robertson, M.C., 2020. Creation of a mixed-mode fracture network at meso-scale through hydraulic fracturing and shear stimulation. *Journal of Geophysical Research: Solid Earth*, p.e2020JB019807.

Schwering, P.C., Knox, H.A., Hoots, C.R., Linneman, D., Ajo-Franklin, J. and the EGS Collab Team, 2018. The EGS Collab Hydrofracture Experiment at the Sanford Underground Research Facility – Campaign Cross-Borehole Seismic Characterization. *GRC Transactions*, Reno, NV, pp. 10.

Schwering, P. C., T. W. Doe, W. M. Roggenthen, G. H. Neupane, H. Johnston, P. F. Dobson, . . . C. Reimers (2020), Deterministic Discrete Fracture Network (DFN) Model for the EGS Collab Project on the 4850 Level of the Sanford Underground Research Facility (SURF), paper presented at 54th U.S. Rock Mechanics/Geomechanics Symposium, American Rock Mechanics Association, 2020/9/18.

Settgast, R.R., Fu, P., Walsh, S.D., White, J.A., Annavarapu, C. and Ryerson, F.J., 2017. A fully coupled method for massively parallel simulation of hydraulically driven fractures in 3-dimensions. *International Journal for Numerical and Analytical Methods in Geomechanics*, 41(5), 627-653.

Ulrich, C., Dobson, P.F., Kneafsey, T.J., Roggenthen, W.M., Uzunlar, N., Doe, T.W., Neupane, G., Podgorney, R., Schwering, P., Frash, L., Singh, A. and the EGS Collab Team, 2018. The Distribution, Orientation, and Characteristics of Natural Fractures for Experiment 1 of the EGS Collab Project, Sanford Underground Research Facility. 52nd U.S. Rock Mechanics/Geomechanics Symposium, Seattle, Washington, pp. 8.

Villiger, L., Gischig, S., Doetsch, J., Krietsch, H., Dutler, O., Jalali, M., Valley, B., Selvadurai, P.A., Mignan, A., Plenkers, K. and Giardini, D., 2020. Influence of reservoir geology on seismic response during decameter-scale hydraulic stimulations in crystalline rock. *Solid Earth,* 11(2), 627-655.

Wang, C., P. Winterfeld, B. Johnston, and Y.-S. Wu (2018), An Embedded 3D Fracture Modeling Approach for Simulating Fracture-Dominated Fluid Flow and Heat Transfer in Geothermal Reservoirs, paper presented at 43rd Workshop on Geothermal Reservoir Engineering, Stanford University, Stanford, California, February 12-14, 2018.

Wang, H.F., Lee, M.Y., Doe, T.W., Haimson, B.C., Oldenburg, C.M. and Dobson, P.F., 2017. In-Situ Stress Measurement at 1550-Meters Depth at the kISMET Test Site in Lead, S.D. 51st U.S. Rock Mechanics/Geomechanics Symposium. American Rock Mechanics Association, San Francisco, California, USA.

Weers, J. and Huggins, J., 2019. Getting Data Out of the Ground: Modern Challenges Facing EGS Collab, the DOE Geothermal Data Repository, and the Geothermal Industry, 44th Workshop on Geothermal Reservoir Engineering, Stanford University, Stanford, California.

White, M.D., Fu, P., Ghassemi, A., Huang, H., Rutqvist, J. and Johnston, B., 2018. Numerical simulation applications in the design of EGS Collab Experiment 1. Proceedings, 43rd Workshop on Geothermal Reservoir Engineering, Stanford, California.

White, M., Johnson, T., Kneafsey, T., Blankenship, D., Fu, P., Wu, H., Ghassemi, A., Lu, J., Huang, H., Neupane, G., Oldenburg, C., Doughty, C., Johnston, B., Winterfeld, P., Pollyea, R., Jayne, R., Hawkins, A., Zhang, Y. and the EGS Collab Team, 2019. The Necessity for Iteration in the Application of Numerical Simulation to EGS: Examples from the EGS Collab Test Bed 1. Proceedings, 44th Workshop on Geothermal Reservoir Engineering, Stanford, California.

Winterfeld, P., B. Johnston, K. Beckers, Y.-S. Wu, and EGS Collab Team, 2019. Code modifications for modeling chemical tracers and embedded natural fractures at EGS Collab. Proceedings, 44th Workshop on Geothermal Reservoir Engineering, Stanford, California.

Wu, H., Fu, P., Yang, X., Morris, J.P. and the EGS Collab Team, 2018. Imaging hydraulic fracture extents and aperture using electrical resistivity tomography, PROCEEDINGS, 43rd Workshop on Geothermal Reservoir Engineering, Stanford, California.

Wu, H., Fu, P.C., Morris, J.P., Settgast, R.R., Ryerson, F.J., Mattson, E.M., Hawkins, A.J. and Zhang, Y.R., 2019a. Stochastic modeling of a conservative tracer test in EGS Collab Experiment 1. 53rd US Rock Mechanics/Geomechanics Symposium. American Rock Mechanics Association, New York, NY, USA, pp. 6.

Wu, H., P. Fu, J. P. Morris, E. D. Mattson, A. J. Hawkins, Y. Zhang, R. R. Settgast, F. J. Ryerson, and E. C. Team, 2019b. Characterizing fracture flow in EGS Collab experiment based on stochastic modeling of tracer recovery. 44th Workshop on Geothermal Reservoir Engineering, Stanford, California.

Wu, Y.S., Yu, X., Wang, S., Wang, C., Winterfeld, P. and EGS Collab Team, 2020. Modeling thermal-hydrologic-mechanical processes for EGS Collab thermal circulation tests using embedded discrete fracture model. 45th Workshop on Geothermal Reservoir Engineering, Stanford, California.

Wu, H. Fu, P., Morris, J.P., Mattson, E.D., Neupane, G., Smith, M.M., Hawkins, A.J., Zhang, Y., Kneafsey, T., and the EGS Collab Team, 2021. Characterization of flow and transport in a fracture network at the EGS Collab field experiment through stochastic modeling of tracer recovery. *Journal of Hydrology, 593, 125888*.

Ye, Z., Vachaparampil, A., Zhou, X., Ghassemi, A. and Kneafsey, T., 2019. Failure Behavior of the Poorman Schist and Its Fractures from EGS Collab Stimulation Site. 44th Workshop on Geothermal Reservoir Engineering, Stanford, California.

Yildirim, E.C., Im, K., Elsworth, D. and the EGS Collab Team, 2018. Co-evolution of fracture permeability and friction in rocks from the EGS Collab Experiment 1 Site. 52nd U.S. Rock Mechanics/Geomechanics Symposium. American Rock Mechanics Association, Seattle, Washington, pp. 8.

Zang, A., Stephansson, O., Stenberg, L., Plenkers, K., Specht, S., Milkereit, C., Schill, E., Kwiatek, G., Dresen, G., Zimmermann, G. and Dahm, T., 2017. Hydraulic fracture monitoring in hard rock at 410 m depth with an advanced fluid-injection protocol and extensive sensor array. *Geophysical Journal International*, 208(2), 790-813.

Zhang, Y., Doughty, C., Pan, L., Kneafsey, T. and Egs Collab Team, 2018. What could we see at the production well before the thermal breakthrough? Proceedings, 43rd Workshop on Geothermal Reservoir Engineering, Stanford, California.

Zhang, Y., Dekas, A.E., Hawkins, A.J., Parada, A.E., Gorbatenko, O., Li, K. and Horne, R.N., 2020. Microbial Community Composition in Deep-Subsurface Reservoir Fluids Reveals Natural Interwell Connectivity. *Water Resources Research*, 56(2), p.e2019WR025916.

Zhou, J., Huang, H., Mattson, E., Wang, H.F., Haimson, B.C., Doe, T.W., Oldenburg, C.M. and Dobson, P.F., 2017. Modeling of hydraulic fracture propagation at the kISMET site using a fully coupled 3D network-flow and quasi-static discrete element model. Proceedings, 42nd Workshop on Geothermal Reservoir Engineering, Stanford, California.

Zhou, Q., Oldenburg, C.M., Kneafsey, T.J. and the EGS Collab Team, 2018. Modeling transport of multiple tracers in hydraulic fractures at the EGS Collab Test Site. Proceedings, 43rd Workshop on Geothermal Reservoir Engineering, Stanford, California. Proceedings, 42nd Workshop on Geothermal Reservoir Engineering, Stanford, California

Zhu, W., & Beroza, G. C. (2018). PhaseNet: A Deep-Neural-Network-Based Seismic Arrival Time Picking Method. *Geophysical Journal International*. 216, 261-273.